Markolin Philipp, Bakk. rer. nat.

Post-translational regulation of adipose triglyceride lipase

Masterarbeit

zur Erlangung des akademischen Grades
Master of Science
an der Naturwissenschaftlichen Fakultät der
Karl-Franzens-Universität Graz

Begutachter

Ass. Prof. Dr. Mag. Günter Hämmerle
Institut für Molekulare Biowissenschaften
Karl-Franzens-Universität Graz

2013

Acknowledgement

I would like to thank Dr. Günter Hämmerle for giving me the chance to work on my own project and for his constant support and supervision. I am grateful to Dr. Rudolf Zechner for recruiting and integrating me in his laboratory.

This thesis would not have been possible without the constant support and occasional guidance from the whole laboratory group, especially Doris Jäger, Kathrin Zierler and Nina Pollak, who continuously helped with new methods and provided their expertise. I would also like to mention Tarek Mustafa and Martina Schweiger and thank them for their help and critical advice on my project.

Finally, I am really happy and grateful that I had the chance to experience such an extraordinary time during my studies and research, what would not have been possible without the support from my parents and friends.

Abstract

In times of plenty, when food intake provides more energy than is needed immediately, animals temporarily store the excess energy as triacylglycerol (TG) predominantly in adipose tissue. On energy demand, the adipose tissue TG stores are mobilized in a process called lipolysis and the generated fatty acids (FAs) are supplied to various tissues including the heart and liver.

Adipose triglyceride lipase (ATGL) is the rate-limiting enzyme responsible for the hydrolysis of TG deposited in both, adipose and non-adipose tissue. Comparative gene identification 58 (CGI-58) is a co-activator protein of ATGL and increases ATGL activity up to 20-fold, which is necessary for full TG hydrolase activity *in vivo* and *in vitro*. Both, CGI-58 and ATGL are crucial for lipolysis while loss-of-function mutations in CGI-58 and/or ATGL in mammals are associated with excessive and ectopic lipid accumulation, which is causative for many illnesses such as hepatic steatosis, cardiac insufficiency and lethal cardiomyopathy.

For the characterization of the tissue-specific role of CGI-58 in lipid catabolism, Dr. Kathrin Zierler at the Institute of Molecular Biosciences generated and characterized mice lacking CGI-58 in muscle and liver. Dr. Zierler could show that muscle specific CGI-58 knock-out (mCGI-58KO) mice exhibit markedly elevated ATGL protein levels in heart and skeletal muscle, possibly to counterbalance for the loss of TG hydrolase activity caused by CGI-58 deficiency. Even more remarkably, ATGL mRNA levels are decreased in CGI-58 deficient cardiac muscle, suggesting a mechanism which promotes stabilization of ATGL protein rather than an increase in ATGL protein expression. Furthermore, ATGL accumulation can be induced *in vitro* (mRNA independently) by AMPK activation via 5-aminoimidazole-4-carboxamide ribonucleotid (AICAR) or treatment with the proteasome-specific inhibitor MG132. Taken together, these findings suggest a post-translational regulation of ATGL stability, but despite its crucial role in lipid metabolism and whole body energy homeostasis, up to now only little is known about post-translational regulation of ATGL *in vivo*.

Curiously, ATGL accumulation is most pronounced in oxidative tissues like heart and muscle, which might argue for an oxidative tissue specific regulation of lipolysis, at least in the pathological mCGI-58KO system.

In summary, the present study addresses the post-translational regulation of ATGL protein stability and also the critical role of ATGL in maintaining energy homeostasis in oxidative tissue.

Table of contents

1) Introduction

2) Materials

3) Methods

1) Introduction

1.1 Obesity, diabetes and metabolic syndrome as new age diseases

The world health organisation (WHO) describes obesity as one of the most blatantly visible, yet most neglected, public-health problem that threatens to overwhelm both more and less developed countries [1]. The problems of overweight and obesity have achieved global recognition only during the past 10 years, in contrast to underweight, malnutrition, and infectious diseases, which have always dominated thinking.

The WHO now accepts a body-mass index (BMI) of 25.0 kg/m^2 or higher as abnormal; the overweight category is classified as obese when the BMI is 30.0 kg/m^2 or more [2]. The risks of diabetes, hypertension, and dyslipidaemia increase from a BMI of about 21.0 kg/m^2 [3]. Excess bodyweight is now the sixth most important risk factor contributing to the overall burden of disease worldwide [4] with 1.1 billion adults and 10% of children who are now classified as overweight or obese.

The major causes of death associated with obesity are coronary artery disease (mainly heart disease, and stroke), Type 2 diabetes, hepatic steatosis, musculoskeletal disorders (especially osteoarthritis), some cancers (-endometrial, -breast, and coloncancer), hypertension, sleeping problems, and polycystic ovarian syndrome [5].

Many of the co-morbidities of obesity are also reflected in the so-called metabolic syndrome, originally defined arbitrarily by WHO on the basis of insulin resistance with other features of obesity or pragmatically on the basis of three of five features: hypertension, large waist circumference, abnormal concentrations of triglycerides, HDL cholesterol and fasting glucose [6, 7].

Obesity is rapidly increasing all over the world. The WHO predicts that in 2015 approximately 2.3 billion adults will be overweight and more than 700 million will be obese [8], which is not only a challenge for social and medical systems, but also urge scientist to provide insight into mechanisms leading to these illnesses.

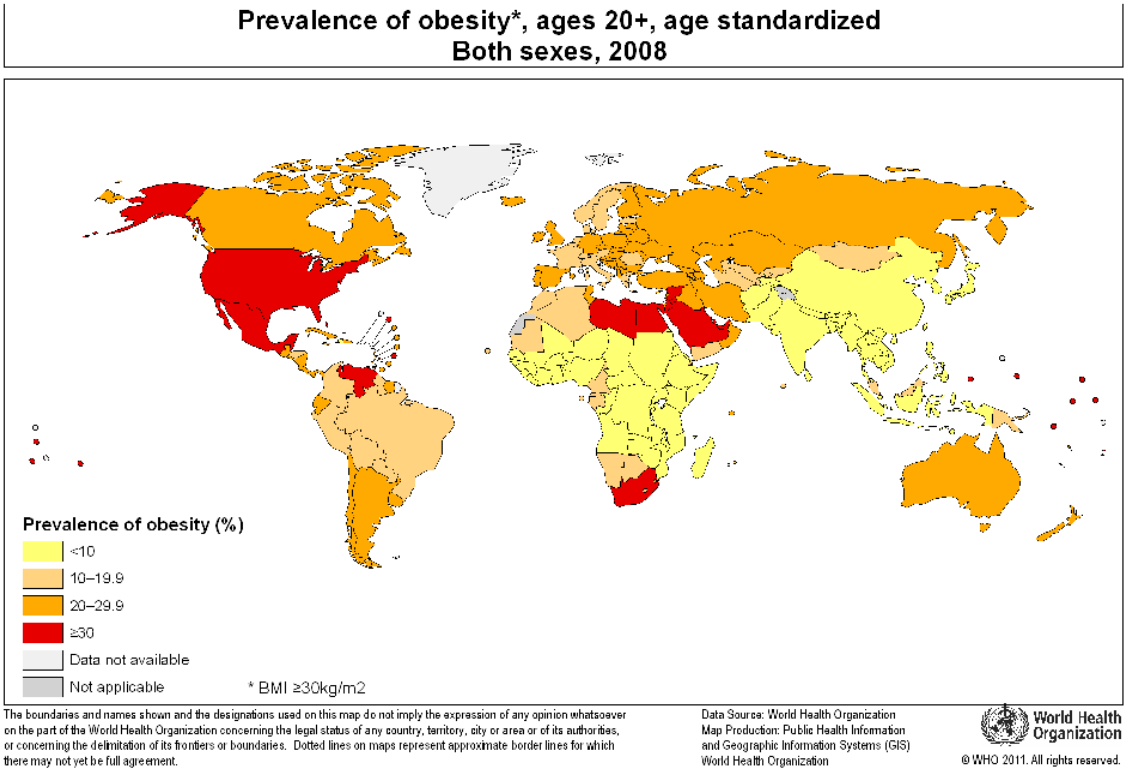

Figure 1.1 A graph depicting the p**revalence of obesity in the world population 2008** *http://www.hsph.harvard.edu/obesity-prevention-source/obesity-trends/map-of-global-obesity-trends/index.html*04/Apr/2011, accessed 28/2/2013

1.2 The metabolic basis of disease

Diabetes, obesity, metabolic syndrome and many other diseases derive from a common precursor condition, which is a deregulation or dysfunction in lipid metabolism. While the prevalence of these diseases is ubiquitous and on the rise, only just recently we began to understand the principles of lipid metabolism in health and disease on a molecular basis. Evidently, we need to consider not only the complex interplay of mechanisms within the cell, but also between tissues and the whole organism, to comprehend the initiation and facilitation of a plethora of illnesses.

Solely a profound and integrative understanding of how the body reacts to and regulates ever-changing nutrient and environmental conditions will provide scientists the tools to combat these new age diseases.

1.3 Obesity as a major cause of cardiac hypertrophy and cardiovascular disease

Cardiovascular disease remains the number one cause of mortality in the Western world, with heart failure representing the fastest growing subclass over the past decade [9]. Obesity is a major contributor to the development of cardiovascular disease as it results in increased risk for hyperlipidemia and ectopic fat accumulation in non-adipose tissues among a plethora of other co-morbidities.

Furthermore, ectopic fat accumulation is accompanied by the development of insulin resistance and consequently Type 2 diabetes [10] andit has been shown to affect cardiovascular function and may contribute to the development of cardiovascular disease [11].

To understand the molecular mechanism by which obesity promotes the development of cardiac disease, it is important to define the pathways leading to fat accumulation in the heart and other tissues.Metabolic alterations, such as (1) decreased fatty acid (FA) β-oxidation, (2) increased FA synthesis due to up-regulation of lipogenic pathways, (3) increased delivery of FAs from adipose tissue and/or (4) defects in TG catabolism may be involved in the development of cardiac hypertrophy as well as genetic predisposition and alteration in signaling pathways [12-15].

1.4 FA processing in adipose and non-adipose tissue

FAs are essential molecules with multiple biological functions; they are integral components of membrane lipids, efficient energy substrates, and potent second messengers [16]. The limited water solubility of FAs and their relatively low critical micellar concentration cause them to form micelles which can adversely affect membrane and cell function. To prevent the deleterious effects of high extracellular or intracellular FA concentrations, long chain FAs are ‘‘detoxified’’ by esterification to glycerol, a trivalent alcohol, forming relatively inert triglycerides (TG). [16]

In times of plenty, when food intake provides more energy than is needed immediately, animals temporarily store the excess energy as TG, the primary constituent of fat, predominantly in adipose tissue (AT).

While white AT is the most important organ to store fatty acids and resupply the circulation with FAs, AT is also able to produce and secrete adipokines such as leptin, adiponectin, resistin and many others, which are involved in regulating lipid and carbohydrate metabolism, appetite and energy expenditure [16, 17], further underlining the important role of AT to maintain whole body energy homeostasis.

During fasting or starvation, the TG stored in AT are hydrolysed and the generated non-esterified “free” fatty acids (FFA) are released into circulation [15] to supply essentially all other tissues with energy substrate.

In the past few decades it has become clear that various membrane-associated fatty acid-binding proteins facilitate the cellular entry of FAs, which are then accepted by cytoplasmic FA binding proteins (FABPc). Furthermore, it has been found that acute changes in FA uptake in response to mechanical (e.g., muscle contraction) and hormonal stimuli (insulin) are regulated by specific membrane proteins, in a fashion similar to the regulation of glucose uptake by glucose transporters. For instance, muscle contraction, through activation of AMP kinase, increases the translocation of FA transporters (CD36) to the sarcolemma to increase FA uptake, and concomitantly increases mitochondrial FAß-oxidation to produce ATP needed to sustain contraction [17]. Evidently, proper functioning of FA transport as well as regulation of the intracellular FFA concentration is tightly controlled by the balance between TG hydrolysis and FFA re-esterification [18-20].

1.5 Lipid droplets are unique cellular organelles

AT is not the only organ able to store TG, in fact, every cell is capable to store neutral lipids in the form of lipid droplets (LD) in more or less quantities. LD are unique cellular organelles consisting of a lipid core enclosed by a phospholipid monolayer [21]. The protein components of LD have been excessively studied over the past decade, identifying the perilipin protein family as the most abundant proteins coating

LD [22]. Perilipins interact with both, lipid and cytosolic proteins, thereby forming an amphipathic interface between to stored lipids and the cytosol. Furthermore, and even more importantly, perilipins have been shown to interact with cellular lipases, thereby interfering with TG mobilization by regulating access of neutral lipid lipases like adipose triglyceride lipase (ATGL) and hormone-sensitive lipase (HSL) to their lipid substrates [23-26]. LD in the cells of various vertebrate tissues are coated with two to four types of perilipin, suggesting that each unique combination imparts tissue specific management of lipid metabolism [27].

1.6 Lipolysis and lipases in TG catabolism

One of the most important steps in response to starvation or malnutrition is the breakdown of TG into FFA and glycerol, a highly coordinated 3-step process called lipolysis. The generated FFAs are utilized as fuel for ß-oxidation in the mitochondria, finally providing adenosine-5'-triphosphate (ATP), the energy currency of the body. Due to its importance in life, lipolysis is highly regulated by a multitude of factors, while deregulation is associated with diseases such as obesity or Type 2 diabetes. On a molecular level, several lipases and other proteins involved in lipolysis have been identified so far [reviewed in 28, 57].

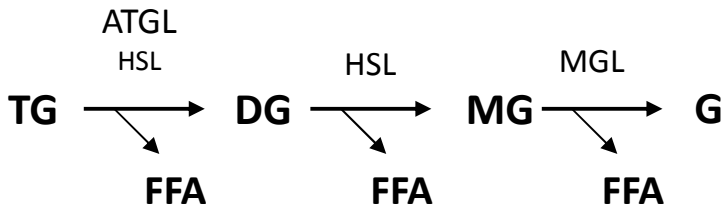

Figure 1.6 **Schematic delineation of the coordinate breakdown of TG.** ATGL catalyzes the first and initial step in TG hydrolysis thereby generating diacylglycerols (DG). Subsequently, DG are hydrolyzed by the enzymatic activity of HSL and the generated monoacylglycerols (MG) are hydrolyzed by both, HSL and monoacylglycerol lipase (MG) to generate glycerol and FFAs.
Abbreviations: ATGL, adipose triacylglycerol lipase; DG, diacylglycerol; G, glycerol; HSL, hormone-sensitive lipase; MG, monoacylglycerol; MGL, monoacylglycerollipase; FFA, free fatty acid; TG, triacylglycerol (Lass A. *et al*, Progress in Lipid Research, 2011)

1.6.1 Adipose triglyceride lipase (ATGL)

Adipose triglyceride lipase (ATGL) was first cloned from a murine AT cDNA and COS-7 cell lysates transfected with an ATGL expressing vector showed a marked increase in TG hydrolytic activity [29]. ATGL is most abundantly, but not exclusively, expressed in white and brown AT. In fact, it has been shown that ATGL is expressed in virtually all tissues, where it selectively performs the first step of TG hydrolysis, generating diacylglycerols (DG) and FFA. Compared to the high enzymatic activity towards TG, ATGL exhibits merely minor or no activity in hydrolyzing other lipid substrates such as DG and MG or retinyl esters [29]. Functional studies revealed that humanATGL acts through a catalytic dyad composed of Ser47 and Asp166 in a canonical GXSXG sequence motive, while substitution of this residues with alanine led to a catalytically inactive enzyme [30,31]. This GXSXG motif is part of the larger patatin-domain which comprises 180 AA and is embedded within a 250 AA α-β-α sandwich structure at the protein's NH_2-terminal half. The COOH-terminal half has a predominant regulatory function and contains a predicted hydrophobic region for LD binding. Curiously, the loss of this region increases the specific *in vitro* activity of ATGL against artificial TG substrates but blunts the intracellular activity due to the inability of the truncated enzyme to bind to cellular LDs [32,33,56].

The central role of ATGL in TG catabolism became obvious by the generation and characterization of ATGL-deficient mice. The lack of ATGL led to ectopic lipid accumulation in various tissues, an increase in whole body fat mass by more than two-fold and a drastic reduction in the life span compared to wild type mice. The most severe consequences of ectopic TG accumulation was observed in the heart, where ATGL deficiency led to a twenty-fold increase in cardiac TG, severe cardiac steatosis and reduced FA availability, consequently promoting a switch to carbohydrates as energy substrates [34]. Furthermore, it has been shown that ATGL deficiency in cardiac muscle disrupts peroxisome-proliferator activated receptor α (PPARα)-induced mRNA expression of genes implicated in FA-oxidation, severely impairs mitochondrial function and finally causes cardiac failure [35]. Humans

affected by ATGL gene mutations develop neutral lipid storage disease (NLSD) with myopathy (NLSDM) [36], which in severe cases requires heart transplantation at an early age.

1.6.2 Comparative gene identification-58 (CGI-58) and G0/G1 switch gene-2 (G0S2) regulate ATGL enzymatic activity

ATGL enzymatic activity is determined by the interaction with the co-activator CGI-58 [30]. CGI-58 is ubiquitously expressed and the highest expression levels were found in adipose tissue, and testis [30]. CGI-58 is a member of the esterase/thioesterase/lipase subfamily of proteins with α/β hydrolase folds, however the putative nucleophilic serine within the canonical esterase/lipase GXSXG motive is exchanged with an asparagine, thus rendering CGI-58 itself catalytically inactive. Nevertheless, two laboratories showed that CGI-58, at least *in vitro,* exhibits acylCoA-dependent acylglycerol-3-phosphate acyltransferase (AGPAT) activity [37,38] but the physiological impact of this observation remains to be elucidated.

CGI-58 most likely interacts with the NH_2-terminal patatin-domain of ATGL but it is currently unknown, whether CGI-58 interaction induces a conformational change in ATGL structure, efficiently funnels substrates to its active side or even facilitates product removal from the ATGL catalytic side. However, this interaction by itself is not sufficient for ATGL activation because CGI-58 variants, which were capable of binding ATGL, failed to stimulate enzyme activity [39]. ATGL activation in living cells additionally requires the binding of CGI-58 to the LD. Truncated variants of CGI-58, which fail to localize to the LD, but bind to ATGL, are unable to stimulate ATGL activity [39].

Maximal ATGL stimulation is achieved at approximately equimolar concentrations of enzyme and co-activator protein [30] and activation of ATGL by CGI-58 is absolutely necessary to maintain physiologic function *in vivo* [40,41].

Similar to ATGL deficiency, mutant forms of CGI-58 carrying point mutations or protein truncations have been identified as causative for NLSD but interestingly CGI-58 deficiency differs in its clinical appearance in some aspects. CGI-58 mutations cause a

severe skin barrier defect in humans and mice [42,43] and accordingly the disease was designated as NLSD with ichthyosis (NLSDI) formerly annotated Chanarin-Dorfman syndrome [44,45]. Mutant forms of CGI-58 associated with NLSDI lose their ability to activate ATGL and some mutants are primarily located in the cytosol and lose their functional interaction with ATGL [40]. These data indicate that TG accumulation in CDS is caused by defective ATGL activation [34], but does not exclude an ATGL-independent function for CGI-58.

Recently, a protein called G0S2 was identified as a selective inhibitor of ATGL [46]. G0S2 was originally found to be expressed during re-entry of blood mononuclear cells from G0 into G1 phase of the cell cycle [47], but has now been demonstrated that G0S2 is predominantly expressed in AT and liver and that overexpression of G0S2 in cells causes massive lipid accumulation. G0S2 directly interacts with the patatin-domain of ATGL similar to CGI-58, but does not compete with CGI-58. G0S2 is expressed ubiquitously and was shown to be induced by insulin and inhibited by tumor necrosis factor α (TNFα) and isoproterenol, both factors that stimulate lipolysis [48]. Furthermore, G0S2 was found to be a PPARγ target gene containing a PPAR-response element (PPRE) in its promoter sequence. In contrast to PPARγ, PPARα down-regulates G0S2 mRNA expression [48], further undermining its regulatory role in lipid metabolism.

1.6.3 Hormone-sensitive lipase (HSL) and monoglyceride lipase (MGL) in TG catabolism

In contrast to ATGL, HSL has broad substrate specificity, as the enzyme is able to hydrolyze TG, DG, MG, cholesterol and retinylesters (CE, RE) and other ester substrates [49]. However, HSL exhibits highest enzymatic activity towards the second step in TG catabolism, i.e. the hydrolytic cleavage of DG thereby generating MG and FFA [50]. Besides the GXSXG catalytic site motif commonly found in lipases, HSL shows no homology with other known eukaryotic lipases or proteins. With respect to the conservation of the AAs of the catalytic triad it is assumed that HSL forms an α/β

hydrolase fold with an active site serine [51]. Upon investigation of HSL deficient mice, it was surprising that the animals were not overweight or obese, but showed decreased WAT weight and were resistant to diet-induced obesity [52]. Notably, HSL-deficiency caused marked DG accumulation in several tissues, establishing HSL as the rate-limiting lipase for DG hydrolysis *in vivo* [50].

MGL was first isolated from rat AT and was shown to specifically hydrolyze MG but not TG or DG [53]. Since then, MG was assumed to be responsible for the third step in TG catabolism, the conversion of MG to glycerol and FFA. Recently, the 3D structure of MG has been determined [54]. MGL also belongs to the large superfamily of α/β-hydrolase fold proteins with a GXSXG motif. The catalytic triad is composed by Ser122, Asp239, and His269. MGL mRNA levels are particularly high in adipose tissue, kidney, and testis, yet the importance of MGL in hydrolyzing MG derived from TG breakdown has only recently been addressed [115].
However, there is emerging evidence that MGL might have a pivotal role in endocannabinoid signaling as MGL deficient mice exhibit elevated MG species enriched in the brain [55]. If other MG hydrolases like HSL or α/β-hydrolase domain-containing 6 (ABHD6) are also relevant for MG hydrolysis *in vivo* remains to be explored.

1.7 Regulation of lipolysis

1.7.1 Transcriptional regulation

ATGL mRNA expression pattern is relatively well characterized and influenced by numerous effectors and conditions. For example, the enzyme is upregulated during adipose differentiation and a target for the transcription factors PPARγ and insulin-responsive transcription factor forkhead box O1 (FoxO1). Furthermore, glucocorticoids such as dexamethasone, the PPARγ agonists thiazolidinediones and also fasting induce mRNA expression. In contrast, insulin, TNF-α, mTOR complex 1 and obviously feeding repress ATGL mRNA expression [reviewed in 28,57].

Interestingly, the ß-adrenergic agonist isoproterenol and also TNF-α reduce ATGL (and HSL) mRNA levels in adipocytes [58] but, conversely, stimulate lipase activities and FA and glycerol release. The discrepancy between lipase mRNA levels and activities is explained by the extensive posttranslational regulation of ATGL and HSL, thus rendering cellular lipase mRNA levels inadequate as indicators of enzyme activities.

1.7.2 Post-translational regulation

In contrast to ATGL, post-translational regulation of HSL has been intensively studied and is best characterized in adipocytes [59-63]. Shortly, adipose HSL activity induced by ß-adrenergic stimulation is controlled by two distinct mechanisms:
(1) The enzyme is phosphorylated by cAMP-dependent protein kinase A (PKA), which leads to a two-fold increase in activity and (2) phosphorylated HSL interacts with perilipin-1, which itself is also a target for PKA phosphorylation. Interestingly, the phosphorylation of HSL induces the translocalization of HSL to the LD surface, mediated by phosphorylated perlipin-1. In contrast, in the basal, non-hormonally stimulated state, perlipin-1 is not phosphorylated and prevents binding of HSL to the LD. After full hormonal stimulation, the combined action of phosphorylated perlipin-1 mediated LD translocation and phosphorylation of HSL causes a 100-fold induction in HSL activity.

Compared to HSL, ATGL posttranslational regulation is not PKA dependent, although ATGL can be phosphorylated at two serine residues [64]. However, unlike HSL, ATGL requires a co-activator protein, CGI-58, for full hydrolase activity and is also specifically inhibited by the small protein G0S2. LD associated proteins like perlipin-1 also participate in the regulation of ATGL in AT, by binding to CGI-58 and thus preventing induction of ATGL activity under non-stimulated conditions [65,66].

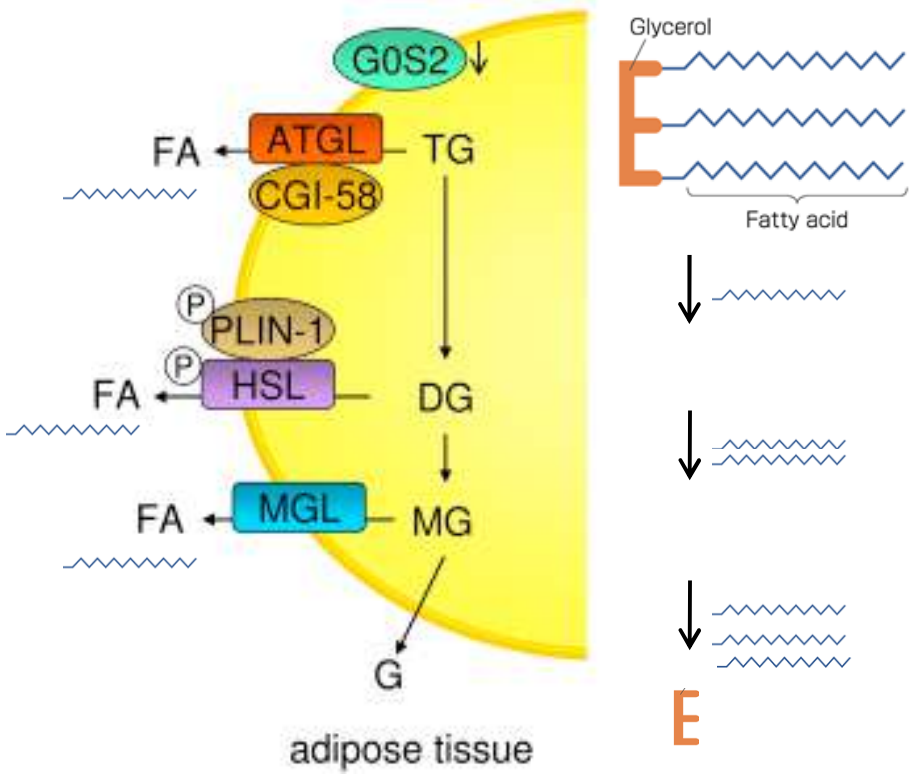

Figure 1.7.2 **AT lipolysis is a complex and highly regulated process.**
Beta-adrenergic stimulation of lipolysis leads to the consecutive hydrolysis of TG and the formation of FAs and glycerol. The process requires three enzymes: ATGL cleaves the first esterbond in TG, HSL hydrolyzes specifically DG, and MGL finally generates MG. For full hydrolytic activity, ATGL interacts with its co-activator protein CGI-58, whereas HSL is phosphorylated and translocates to the LD upon PLIN-1 phosphorylation. Expression of the ATGL inhibitor G0S2 during fasting is low in adipose and high in oxidative tissues.
Abbreviations: ATGL, adipose triglyceride lipase; CGI-58, comparative gene identification-58; DG, diacylglycerols; FA, fatty acid; G, glycerol; G0S2, G0/G1 switch gene 2; HSL, hormone-sensitive lipase; MG, monoacylglycerols; MGL, monoglyceride lipase; PLIN-1, perilipin-1; PLIN-5, perilipin-5; TG, triacylglycerol (Zechner R et al., Cell Metabolism, 2012)

1.8 The ubiquitin-proteasome system

Ubiquitination is a multi-step process where a small 8.5 kDa ubiquitin protein is covalently attached to a lysine residue of a targeted protein substrate mediated by an ATP-dependant enzymatic cascade involving an ubiquitin-activating enzyme (E1), an ubiquitin-conjugating enzyme (E2), and an ubiquitin-ligase (E3) [67-69]. While the resulting mono-ubiquitinated proteins are shown to have some unique roles in various cellular functions [70], mono-ubiquitination commonly provides a platform for consecutive ubiquitination events, leading to the formation of poly-ubiquitin chains and marks the targeted protein for proteasomal degradation [71].

The eukaryotic proteasome is an approximately 2.5 MDa multimeric complex consisting of more than 31 subunits forming a hollow cylindrical structure and was first described as high molecular weight alkaline protease [72]. As a multicatalytic protease, it is characterized by three major activities with distinct specificities against peptide substrates namely tryptic-, chymotryptic-, and peptidylglutamyl peptide-hydrolytic (PGPH) activities [73], constituting the major extralysosomal protein degradation system [74].

Like phosphorylation, post-translational modification of proteins with ubiquitin can result in the regulation of numerous cellular functions, such as the DNA damage response, apoptosis, cell growth, and the innate immune response; concomitantly proteasomal dysfunction has been linked to disease [75,76].

Recently, studies have described how ubiquitination in the heart regulates key signaling transduction pathways involved in the development of common cardiac diseases, including cardiac hypertrophy, heart failure, ischemia reperfusion injury, and diabetes [77].

Furthermore, there is emerging evidence that the ubiquitin-proteasome system (UPS) regulates many proteins critically involved in lipid metabolism via controlling protein stability and abundance in response to lipolytic or environmental cues [78-81].

1.9 AMP-activated protein kinase (AMPK)

All living cells use ATP as the immediate source of energy. In order to survive, cells need to ensure that they maintain a relatively high and constant level of ATP [82]. Thus, within the individual cell, the demand of ATP must be matched by its supply. For this purpose, the cell needed to develop an ATP sensor, which registers a fall in ATP levels, as well as a means to counteract energy expenditure. One such system that has been identified in eukaryotic cells isthe 5-AMP activated kinase (AMPK) cascade. AMPK is a heterotrimeric protein kinase complex and orthologues are expressed in virtually all eukaryotes. The primary function of AMPK is to monitor changes in the intracellular level of ATP and to couple this to phosphorylation of downstream

substrates leading to an increase in the rate of ATP- producing pathways and/or a decrease in the rate of ATP-utilizing pathways [83].

AMPK is composed of three subunits, α, β and γ, respectively. In mammalian cells, there are two isoforms of the α subunit, two isoforms of the β subunit and 3 isoforms of the γ subunit [84]. The α subunit contains a typical serine/threonine protein kinase domain at the N-terminus and a C-terminal regulatory domain. The primary mode of regulation of AMPK is by reversible phosphorylation of a threonine (Thr172) residue within the activation loop segment of the α subunit [85], which functions as an on-off switch for kinase activity.

The level of Thr172 phosphorylation is determined by the relative activities of the upstream kinases (CaMKKβ and LKB1) and the protein phosphatases acting on AMPK. CaMKKβ is activated by calcium and calmodulin and conditions which increase intracellular calcium lead to an increased phosphorylation of Thr172 [86-88]. In contrast, LKB1 appears to be constitutively active, since its activity is unaffected by treatments that cause a marked increase in AMPK activity [89].

In the last decade, AMPK has been linked to a variety of research areas, particularly cancer and metabolic diseases, energy homeostasis and signal transduction. [90-94]

However, the role of AMPK in regulating lipid metabolism has been controversial and yet to be defined.

In adipocytes, AMPK has been shown to phosphorylate ATGL at two serine residues (S406 and S430), possibly enhancing thehydrolytic activity of ATGL [95]. Interestingly, the amino acid sequence of S406 of ATGL constitutes a canonical 14-3-3 binding motif, bearing the question if the observed increase in lipolytic activity after AMPK stimulation promotes a change in conformation, localization or stability of ATGL upon S406 phosphorylation. Additionally, 5-aminoimidazole-4-carboxamide-1-β-d-ribofuranoside (AICAR), a potent and specific AMPK activator, was reported to increase ATGL protein expression and lipolysis in adipose tissue [96] suggesting a pivotal role for AMPK in regulating ATGL-mediated lipid metabolism.

2) Materials

All chemicals were bought from Sigma, Merck or Roth. Chemicals were solved in distilled, deionised water (DD water) and stored at RT, if not otherwise indicated.

2.1 Buffers

List of commonly used buffers

10% APS:	1 g ammonium persulfate in 10 ml stored at -20°C
30% acrylamide	
30% acrylamide	0.8% bisacrylamide in 500 ml stored at 4°C
4 x lower Tris buffer	0.5 M Tris pH 6.8 stored at 4°C
4 x upper Tris buffer	0.5 M Tris pH 8.8 0.4% SDS stored at 4°C
10 x SDS-Page buffer	200 mM Tris 1.6 M glycine 0.83% SDS
4 x SDS loading buffer	0.2 M Tris pH 6.8 10% β-mercaptoethanol 8% SDS 40% glycerine bromophenol blue (tip of a spatula) stored at -20°C
10 x TST	1% Tween 20 1.5 M sodium chloride 500 mMTris/hydrochloric acid pH 7.4 stored at 4°C
CAPS transfer buffer	10 mM CAPS pH 11 10% methanol

Coomassie blue	0.25% coomassie blue 7.5% from 80% acetic acid 50% ethanol
Destain solution	30% methanol 10% from 80% acetic acid
Potassiumphosphate buffer	1 M KH_2PO_4/K_2HPO_4; pH 7.0
PBS buffer	137 mMNaCl; 2.7 mMKCl; 4.3 mM Na_2HPO_4- 7 H_2O; 1.4 mM KH_2PO_4; pH 7.4
DEPC water	1 ml diethylpyrocarbonate in 1 l water, autoclaved
Buffer A	50 mM Tris pH = 7.8 20 mMKCl 0.5 mMMgOAc 1 mM DTT
Lysis buffer I	Buffer A 20% Glycerol 2 mM ATP
Buffer B	50 mMKaliumphosphat pH 7.4; 100 mMKCl; 1 mM EDTA
Lysis buffer II	0.3 N NaOH; 0.1% SDS
1000 x Pi	1 mg pepstatin 2 mg antipain 20 mg leupeptin in 1 ml stored at -20°C
HSL buffer	0.25 M sucrose pH 7 (with 10% acetic acid) 1 mM EDTA 1 mM DTT in 200 ml stored at -20°C
5 x loading dye	3 ml 30% glycerin 7 ml DD water 25 mg bromophenol blue 25 mg xylen-cyanol stored at -20°C
10x oleic acid	2 mg/ml oleic acid complexed with BSA

2.2 Substrates and Inhibitors

Substrate for TG hydrolase activity measurements	0,27 mg/ml Triolein; 0,15 mg/ml PC:PI (3:1); 12,5 µCi/ml ^{3}H-labeled Triolein
Proteasome fluorogenic substrate	1 µM Suc-Leu-Leu-Val-Tyr-AMC (Enzo Life Sciences GmbH)
Inhibitor of protein biosysnthesis	100 µg/ml Cycloheximide (Sigma Aldrich)
Proteasome-specific inhibitors	10 mM MG132 (Firma)
General protease inhibitors	1000x Leupeptine (Lactan)
Lysosomal inhibitors	10 mMChloroquine (Sigma Aldrich) 100 mM NH_4Cl (Sigma)
USP14-Inhibitor	50 mM USP14-Inhibitor (VWR International)
^{3}H- Labeled Triolein	Triolein, [1-oleoyl-9,10-3H](Humos Diagnostika GmbH)

2.3 Antibodies

anti-N-terminal His antibody	Clontech, Palo Alto, CA,USA
anti-ATGL antibody	New EnglandBiolabs
anti-CGI-58 antibody	AbnovaGmbH
anti-HSL antibody	New EnglandBiolabs
anti-ß-actin antibody	Sigma Aldrich
anti-GAPDH antibody	New EnglandBiolabs
anti-Ubiquitin(K48) antibody	New EnglandBiolabs
anti-mouse IgG	Amersham Biosciences, Buckinghamshire, UK
anti-rabbit IgG	Amersham Biosciences, Buckinghamshire, UK

All primary antibodies were diluted 1:1000 in 5% skimmed milk.
Secondary antibodies were diluted 1:10000 in 5% skimmed milk.

2.4 Standards

Protein Determination Standard: Albumin 2.0 mg/ml (Pierce)

Glycerol Standard Solution: Glycerol 2.5 mg/ml (Sigma)

Cholesterol Standard: Free Cholesterol C 100 mg/dl (Wako Chemicals)

Free Fatty Acid Standard: NEFA C Cal 1.0 mM (Wako Chemicals)

Precision Plus All Blue Protein Standard (BioRad) (Figure)

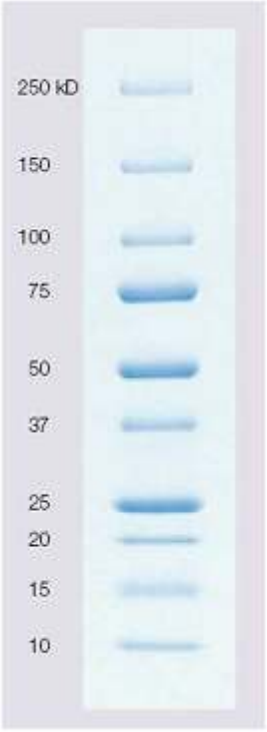

Precision Plus All Blue Protein Standard (BioRad) for SDS-Page

2.5 Enzymes

Used for quantitative reverse-transcriptase (qRT-) PCR

DNase I (Invitrogen)

RNase A (Roche Diagnostics)

SuperScript® III Reverse Transcriptase (Invitrogen)

3) Methods

3.1 Cell culture

3.1.1 Cultivation of Cos7 and H9C2 cells

The cultivation of COS-7 and H9C2 cells was carried out in 175cc culture flasks. Dulbecco's modified Eagle Medium (DMEM, Gibco-Invitrogen, Carlsbad, USA) with 10% fetal calf serum (FCS, Gibco-Invitrogen, Carlsbad, USA), antibiotics (100 µg/ml penicillin and 100 µg/ml streptomycin) and 1,0 g/l or 4,5 g/l glucose for COS-7 and H9C2 cells respectively was used as full media for growth at 37 ° C and 5% CO_2 in an incubator. Any further procedures were carried out in a laminar flow to ensure sterility.

3.1.2 Passaging of cells

Upon reaching 80-90% confluence (to ensure cells were still in the logarithmic phase) the full media was removed and the cells were washed with 10 ml PBS. To detach the cells from the flask surface, they were incubated with 3 ml trypsin solution (trypsin-EDTA 0,05%, Gibco-Invitrogen, Carlsbad, USA) for 2 minutes at 37 ° C. Trypsin is a peptidase used to partially degrade cell adhesion proteins, additionally, cells were removed mechanically from surface with gentle knocking against the flask. Subsequently, the cells were dissolved in 10 ml full media in 50 ml Grainer tubes and centrifuged for 3 min at 1200 rpm. The supernatant was removed and the cells were resuspended in 10 ml full media and subjected to cell counting in Casy-1-Cellcounter (Schärfe System, Reutlingen, Germany).

3.1.3 Transfection of COS-7 cells

One day before transfection, cells were counted and 1.5 * 10^5/well or 9 * 10^5 cells were seeded in a 6-well plate or 10 mm Petri dish, respectively. The full media was substituted shortly before transfection with a serum and antibiotic free (-/-) DMEM

media. 6 µg plasmid-DNA in 300 ml (-/-) media were mixed with 30 µl Metafectene (Biontex GmbH, Munich, Germany) in 300 ml (-/-) media and incubated at RT for 20 min. Metafectene is a polykationic transfection reagens that aggregates with plasmid-DNA and shuttles it into the targeted cells via fusion with their cell membrane. The DNA-metafectene mix was incubated with the cells for 4 hours, 37 ° C and then substituted with full media.

3.1.4 Differentiation of H9C2 cells

For differentiation, confluent H9C2 cells were counted and 2 * 10^5 cells/well were seeded in 6-well plates and incubated with differentiation media (DMEM, 4,5% glucose, (+/+), FCS (1%), 10 nM retinoic acid). The media was changed every second day until differentiation could be observed under the microscope. The differentiated cells assume a branched multinucleated, cardiomyocyte-like phenotype after 5-6 days.

3.1.5 Infection of H9C2 cells

On the day of infection, a corresponding volume of virus-DNA diluted in (-/-) media was calculated according to the following formula:

V … volume of virus-DNA
n … number of cells/well
MOI … „multiplicity of infection“
pfu … „plaque forming units“

$$V = \frac{n * MOI}{pfu}$$

Subsequently, the media was removed and the cells were incubated for 2 hours at 37 ° C with the virus-DNA mix. Finally, the media was changed and the cells were fed with fresh differentiation media for 48 hours before harvesting.

3.1.6 Harvesting of cells

Before harvesting, the cells were washed 3 times with PBS buffer to remove albumin-rich media relics. Afterwards, 2 ml PBS/well was added and cells were scraped from the surface with a cell scraper and transferred to a 15 ml Grainer tube. After centrifugation (3 min, 1300 rpm, 4° C) the supernatant was thrown away and the pellet resuspended in 1 ml PBS again and transferred to an Eppendorf tube. The cells were centrifuged again (5 min, 4000 rpm, 4 ° C) and the supernatant was thrown away. Subsequently, the pellet was resuspended in HSL-buffer substituted with protease inhibitor (pi) mix and sonificated (5 s, 20% amplitude) to break the cell wall. Finally, the cells were centrifuged again (5 min, 4000 rpm, 4 ° C) and the supernatant (= lysate) was transferred to a fresh eppendorf tube and stored at -20 °C.

3.1.7 Cell culture experiments

3.1.7.1 CHX based degradation experiment

Cycloheximide (CHX) is an inhibitor of protein biosynthesis in eukaryotic cells widely used to determine protein half-life. H9C2 cells were incubated with CHX and different inhibitors (MG132 [10 µM], Leupeptine [10 µg/ml], NH_4Cl [10 µM] Chloroquine [50 µM]) and harvested at different timepoints (0, 3, 6, 9, 24, 48 h) after incubation.

3.1.7.2 AMPK stimulation/inhibition

Transfected COS-7 cells were incubated with either 10 mM AICAR (5-aminoimidazole-4-carboxamide-1-β-D-ribofuranoside, AMPK activator) or 5 µM Compound C (Calbiochem/Merck, Whitehouse Station, USA, AMPK inhibitor) for 24 h in cultivation media before harvesting.

3.2 Protein determination

3.2.1 Bradford Protein Assay

To perform Bradford protein assay, cell or tissue lysates were diluted appropriately and 20 µl of the sample were then mixed with 200 µl of the Bio-Rad Protein Assay dye reagent (diluted with dd. H2O 1 to 5, Bio-Rad Laboratories GmbH).
The Albumin Standard (2 mg/ml) was diluted 1:10, 1:20, 1:40, 1:80 and 1:160 and 20 µl of the particular sample buffer were used as blank. All samples, standards and blanks were applied 2 times to decrease pipetting error. The 96-well microtiter plate was incubated at least 5 minutes at RT. The spectrophotometer was set to 595 nm for the measurement.

3.2.2 BCA protein assay

Similar to Bradford assay, the BCA method is a fast and accurate method to determine protein concentration. 20 µl of sample were mixed with 200 µl of the BCATM Protein Assay working reagent. The working reagent is prepared by mixing 50 parts of BCA-TM Reagent A with 1 part of BCA-TM Reagent B. The Albumin Standard (2 mg/ml) was diluted in appropriate concentrations. 20 µl of the particular sample buffer were used as blank. The 96-well microtiter plate was incubated 30 minutes at 37°C. The spectrophotometer was set to 595 nm for the measurement.

3.3 SDS-PAGE

3.3.1 Separation Gel

A clean glass plate, between two spacers and an aluminum silicate plate were placed in position. Four arranged plates were put in the casting stand and pressed together by using clamps. Approximately 30 ml separating gel solution of desired percentage (see table below) were poured between the plates, 2 centimeters from the upper

border were spared for the stacking gel. The separating gel was covered with a layer of butanol to avoid evaporation. After 1 hour the gel was ready for usage.

3.3.2 Stacking Gel

The plates with the separating gel were put into the running tank and fixed with clamps. The spared space between the plates was filled up with stacking gel (see table) and a comb (10 or 15 spaces) was inserted. After 30 minutes the stacking gel was ready to use.

3.3.3 Preparation of protein samples

The desired amounts of the samples were mixed with appropriate volume of 4 x SDS loading buffer and then incubated 10 minutes at 99°C.

3.3.4 Running the gel

1 x SDS-Page buffer was poured into the running tank and the comb was removed. Before loading of the samples, the gel sinks were washed with a syringe to remove gel residues. Afterwards, the gel was loaded with the protein standard (Precision Plus All Blue Protein Standard; 8 µl) and the samples. The gels were running with 30 mA for approximately 50 min under constant water cooling.

3.4 Western Blot Analysis

3.4.1 "Sandwich" construction and blotting

The gel was separated from the glass plate with the help of a spacer. Following this the stacking gel was removed and the separating gel transferred on a filter paper which lay on the top of a spongy pad of the blot module. The PVDF membrane was soaked in methanol before use and was put on top of the gel. Air bubbles were rolled out between the membrane and the gel. Another filter paper and another spongy pad were placed on top of the membrane. After the "spongy pad/filter paper/gel/membrane/filter paper/spongy pad sandwich" had been assembled, the

blot module was closed and put into the blot chamber, which was filled with CAPS transfer buffer. The orientation for the blotting procedure has to be minus pole-gel-membrane-plus pole. The transfer was carried out at 200 mA for 1 hour while water cooling.

3.4.2 Blocking and antibody incubation

The membrane (protein side facing up) was blocked with skimmed dry milk in 1 x TST for at least 2 h on a shaker. Subsequently, the membrane was incubated with the diluted primary antibody (see materials) overnight. The next day, the membrane was washed 3 times with 1 x TST for 10 minutes. Then the membrane was incubated with the diluted secondary antibody for 1 hour and washed again 3 times for 10 minutes. Finally, a tube with 1 ml LumigenTM PS-3 detection reagent Solution A and 25 µl LumigenTM PS-3 detection reagent Solution B from the ECL Plus Western Blotting Detection System (GE Healthcare) was prepared.

3.4.3 Antibody detection

All following steps were carried out in a dark room with infrared light. The membrane was incubated for 1 minute with the detection reagent and placed inside a bag. The bag was placed inside the cartridge and air bubbles were rolled out. A light-sensitive film was placed on top of the membrane and the cartridge closed for development for 10 sec to 5 min, depending on the signal intensity. Afterwards, the film was put in developing solution, washed in water and then placed in the fixation solution, washed in water again and hung up to dry.

3.4.4 Membrane stripping

If necessary, the membrane was stripped of its antibodies by incubating the membrane in stripping buffer (20 ml stripping buffer + 140 µl ß-mercapto-ethanol) at 55 ° C for 20 minutes. The stripped membrane was blocked again with 10% milk in TST and could be proceeded as described in 3.4.2.

3.4.5 Coomassie Blue staining

To check for membrane homogeneity and protein bands, the membrane was dunked 30 seconds in Coomassie Blue and then discolored with destain solution. The membrane was dried under a vent and then digitalized by scanning.

3.5 mRNA isolation and qRT-PCR

3.5.1 mRNA isolation from tissue

Tissues were transferred from cryo tubes to assay tubes (PP 16x100 mm) on dry ice and simultaneously weighted. 100 mg tissue was mixed with 1 ml TRIZOL reagent. The Ultra Turrax^{R} homogenizer was washed accurately with DEPC water previously to use and between all samples and all samples were kept on ice. Homogenized tissues were incubated 5 minutes at RT and 0.1 ml 1-brom-3-chlorpropane (BCP) per ml TRIZOL reagent was added. Reaction mixtures were mixed thoroughly and incubated 15 minutes at RT with head over top mixing in between.

Afterwards the samples were centrifuged at 12 000 g 15 minutes at 4°C and the aqueous supernatants were transferred in new assay tubes and 0.5 ml isopropyl alcohol was added. Reaction mixtures were mixed thoroughly and incubated 10 minutes at RT and then centrifuged again at 12.000 x g for 10 minutes at 4°C. The supernatants were removed and the RNA pellets washed with 1 ml 75% EtOH.

The samples were centrifuged at 7500 g 5 minutes at 4°C the supernatants were removed and the assay tubes inverted on a paper towel and left to dry until the alcohol smell has faded away and dry RNA pellets were transparent. Finally, the pellets were dissolved in DEPC water and transferred to Eppendorf tubes (1.5ml). The concentration of the RNA was analyzed on the Nanodrop spectrophotometer ND-1000 (PEQLAB Biotechnology GmbH).

3.5.2 mRNA isolation from cell culture

Cells were washed 3 times in PBS and then 1 ml/well TRIZOL reagent was added to the 6-well plates. The samples are then transferred into 2 ml tubes and either stored at -20 ° C or proceeded as described in 3.5.1.

3.5.3 cDNA synthesis

1 µg RNA (diluted in 5 µl DEPC water) was mixed with 5 µl 10 x DNase-buffer, 3µl DEPC water and 1 µl DNase and the mix was incubated for 15 minutes at RT under shaking (350 rpm). To inactivate the DNase 1 µl 25 mM EDTA was added to the reaction mixture and incubated 10 minutes at 65°C. Afterwards, the cDNA synthesis reaction mix (10x RT buffer, 2mM dNTP, 10x random primer, 1x RNAse inhibitor, 1x reverse transcriptase) was prepared in PCR tubes and heated with the following program on a thermocycler;

	[°C]	[min]
Step 1	25	10
Step 2	37	120
Step 3	85	5
Step 4	4	-

Then the samples were stored at -20°C.

3.5.4 Quantitative RT-PCR

The cDNA of each sample was diluted 1:25 and 4 µl were added to 16 µl master-mix (10 µl SypGr, 1 µl Primer forward, 1 µl Primer reverse, 4 µl H_2O) in a 96-well plate. The master mix was prepared at a prepared space to avoid contamination. The 96-well plate was centrifuged at 2000 rpm shortly and then subjected to qRT-PCR.

3.6 TG hydrolase activity assay

3.6.1 Sample preparation

Tissue samples were washed with 1 x PBS + 1 mM EDTA and disrupted in HSL buffer using an Ultra Turrax Homogenizer. The samples were always kept on ice and the resulting homogenates were centrifuged at 20.000 x g for 30 min at 4°C. Then the infranatants were collected by using an incandescent needle. The protein concentration was determined using the Bradford reagent. Cell culture samples were harvested as described in 3.1.6.

3.6.2 Preparation of assay substrate

All samples were prepared in a total volume of 100 µl HSL buffer in assay tubes (PP 16x100 mm) and examined as triplets.

The TG hydrolase assay was performed with and without recombinant CGI-58-GST.

Substrate composition (1,67mM) for 100 samples (10 ml):

150 µl Triolein 100 mg/ml

75 µl PC:PI (3:1) 20 mg/ml

125 µCiTriolein [9,10-^{3}H]; 1.25 µCi/sample

The substrate was evaporated under nitrogen to get rid of all solvent. Fresh 100 mM potassium phosphate buffer pH 7 was prepared by mixing 1 M dipotassium hydrogen phosphate buffer with 1 M potassium dihydrogen phosphate buffer (310 µl + 690 µl; dilute to 10 ml). The substrate was sonicated (Vir Sonic Sonicator) 3 times for 30 seconds in 2 ml phosphate buffer and kept on ice for 30 seconds between the sonication intervals. Then further 2 ml of buffer were added and the substrate was sonicated again for 30 seconds. Adding 2 ml of buffer and sonication was done till the needed volume (for 10 ml substrate 7.5 ml of buffer is needed) was reached.

2.5 ml (5%) of 20% FFA free BSA (solved in 100 mM potassium phosphate buffer) were added and the substrate was mixed.

3.6.3 TG hydrolase activity assay

100 µl of substrate were added to each sample and the reaction mixture incubated for 1 hour at 37°C in a water bath under shaking. The reaction was stopped by adding 3.25 ml of MeOH/$CHCl_3$/nHeptan (10/9/7) and 1 ml of 0.1 M K_2CO_3 (pH 10.5 with boric acid). The assay tubes were closed and each sample was vortexed about shortly. After that the samples were centrifuged for 15 minutes at 2300 rpm. 1 ml of the resulting upper phase was transferred into scinti vials and 8 ml of scinti cocktail were added. For determination of specific substrate activity 10 µl and 20 µl of the substrate were also measured.

Correction for calculation (nmol FFA/ h* mg Protein):
The upper phase consists of 2.45 ml but solely 1 ml is counted: * 2.45
71.5 % of total FFA are extracted to the upper phase: / 0.715

3.7 TG content determination

3.7.1 Oleic acid loading

Under normal growth conditions, COS-7 accumulate less TG. Therefore, cells were loaded with oleic acid to form LD, which can then be processed by intracellular or recombinant lipases. TG determination after a certain amount of time then indirectly reflects its TG hydrolytic activity.
Oleic acid was complexed with BSA to a concentration of 4 mM in PBS and mixed thoroughly. Afterwards, COS-7 cells were incubated for 20h with 0.4 mM oleic acid and cultivated under normal conditions.

3.7.2 TG extraction and determination

After loading with oleic acid for 20h, the COS-7 cells were washed with PBS 3x and then TG was extracted with 2 x 800 µl Hexane:Isopropanol (3:2) for 10 min. The solvent was evaporated and the dried TG was resolved in 0.1 % Triton-X 100 by sonicating(Virsonic 475, Virtis, Gardiner, New York, USA) for 5 sec. The fixated cells left after TG extraction were incubated with 1 ml 0.3 M NaOH/0.1% SDS and lysated on a rotating wheel for 4 hours, then protein concentration was determined with BCA assay. The extracted TG were prepared for determination by mixing 10 µl of each sample with 100 µl Infinity TM TriglyceridesReagent (Thermo) in a 96-well plate. Glycerol standard (2.5 mg/ml, Sigma) was dilutedin appropriate concentrations. The 96-well plate wasincubated 10 minutes at 37°C and measured with a spectrophotometer set to 492 nm.

3.8 Proteasome activity assay

3.8.1 Substrate stock preparation

10 mM (100x) Stock solution: 5 mg Suc-L-L-V-T-AMC ([764 g/mol], Enzo Lifesciences) is diluted in 653 µl DMSO.

3.8.2 Tissue preparation

All steps are carried out at 4°C. Tissue samples (fresh or snapfrozen) are homogenized in 500-800µl Lysis buffer I (depending on tissue size) in 2 ml Eppendorf tubes with Ultra-Turrax Homogenizer and centrifuged 30 min at 25000 x g. After centrifugation, the infranatant is taken by punctuating the eppendorf tube with a hot needle and transferred to a fresh Eppendorf tube to remove non-soluble and fatty components.
The crude soluble fraction is kept on ice and total protein concentration is determined with Bradford protein assay. An appropriate amount of protein (50-100 µg) is mixed with Buffer A or Buffer A + MG132 (control) to a final volume of 100 µl in a 96-well

plate. Additional controls: Buffer A (blank), Buffer A + Substrate (autohydrolysis control→"substrate shift")

3.8.3 Fluorimetric assay

The fluorimetric assay is carried out in a 96-well plate (black plate with glass bottom) using a Perkin Elmer LS 50B fluorimeter. To start the reaction, 1 µl substrate is added to 100 µl of diluted tissue sample and fluorescence intensity is measured over time.

Program: well plate reader
Excitation wavelength: 360 nm
Emission wavelength: 460 nm
Excitation/Emission slits: 5.0/5.0 (2.5/2.5 for strong signals)
10-20 cycles
2-5 sec read time
2-5 min/cycle

3.8.4 Data analysis

To effectively compare proteasome activity, the increase in fluorescence intensity over time is used to calculate the maximum "k" of the linear slope. (As the assay starts cold at approximately 4°C, it takes about 3-5 min to reach linearity) The Δk_{max} of the each calculation is taken to compare the respective samples.

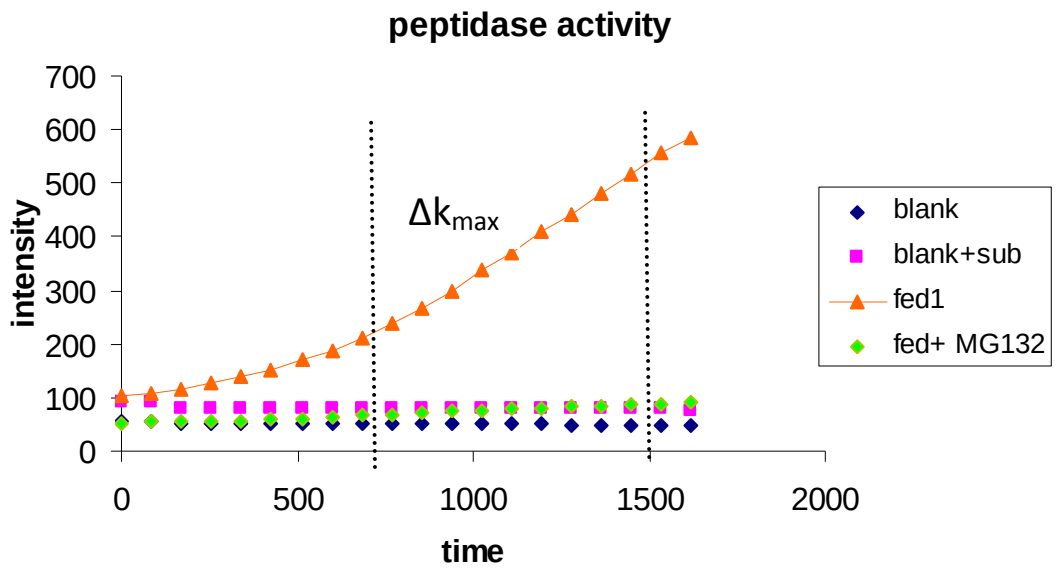

Abbr :	sub…	substrate [Suc-L-L-V-T-AMC]
	fed1…	tissue sample 1 [quadriceps muscle of fed mice]
	fed1 + MG132…	control to estimate unspecific peptidase activity
	Δk_{max} …	maximum gradient of linear slope

3.8 Statistical analysis

All results are indicated with an average ± standard deviation (if n≥3). The significance levels were calculated with the two-tailed Student's t-test (* $p < 0.05$; ** $p < 0.01$; *** $p < 0.001$)

4) Results

4.1 Thesis rationale

4.1.1 ATGL protein level is substantially increased in mice lacking CGI-58 in muscle

Heart homogenates prepared from mice lacking CGI-58 in muscle (hereafter designated as mCGI-58KO mice) and CGI-58 flox/flox or wild type mice (designated CGI-58 f/f wt or wt mice) were subjected to western blotting analysis. Curiously, the ATGL antibody recognizes a second strong band specifically in cardiac muscle (CM).

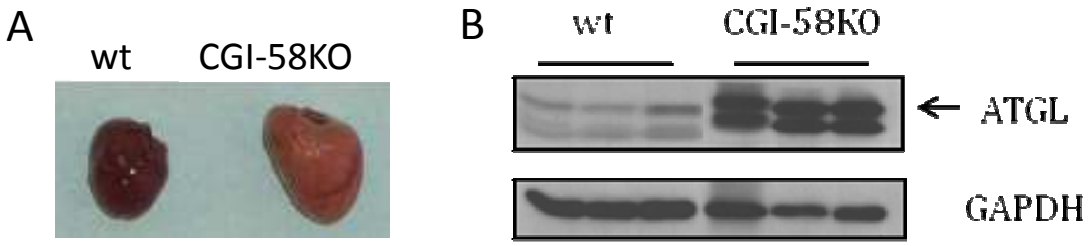

Figure 4.1.1 **ATGL protein level is increased in CM of mCGI-58KO mice** (A) Hearts prepared from CGI-58 flox/flox and mCGI-58KO mice. (B) Western Blot analysis of ATGL protein levels in CM (50 µg) of CGI-58 f/f wt and mCGI-58KO mice. Glyceraldehyde 3-phosphate dehydrogenase (GAPDH) was used as loading control to confirm equal protein loading. ATGL has a molecular weight of 54kDa.

Western blot analysis of ATGL protein levels in CM of mCGI-58KO mice unveiled a massive increase in ATGL protein (10-fold) content in CM compared to wt (figure 4.1.1). This finding suggests that inadequate lipolysis caused by the absence of muscle CGI-58 leads to a compensatory increase in ATGL protein expression levels. However, the increase in ATGL protein levels was not able to compensate impaired TG catabolism in the absence of CGI-58 [97].

4.1.2 mRNA levels of cellular lipases are reduced in CM of mCGI-58KO mice whereas levels were normal in skeletal muscle

To further investigate the cause for increased ATGL protein levels in muscle of mCGI-58KO mice, RNA was isolated from CM and skeletal muscle (SM) of mCGI-58KO and wt

mice. Subsequently, 1 µg tissue RNA was transcribed into cDNA and applied to quantitative RT-PCR.

In CM, the relative mRNA levels of ATGL (- 48%) and also HSL (- 51%) and MGL (- 53%) were significantly reduced in mCGI-58KO mice compared to wild type (figure 4.1.2). However, in SM, merely MGL mRNA levels were mildly decreased (- 22%), which is in line with other observations [97].

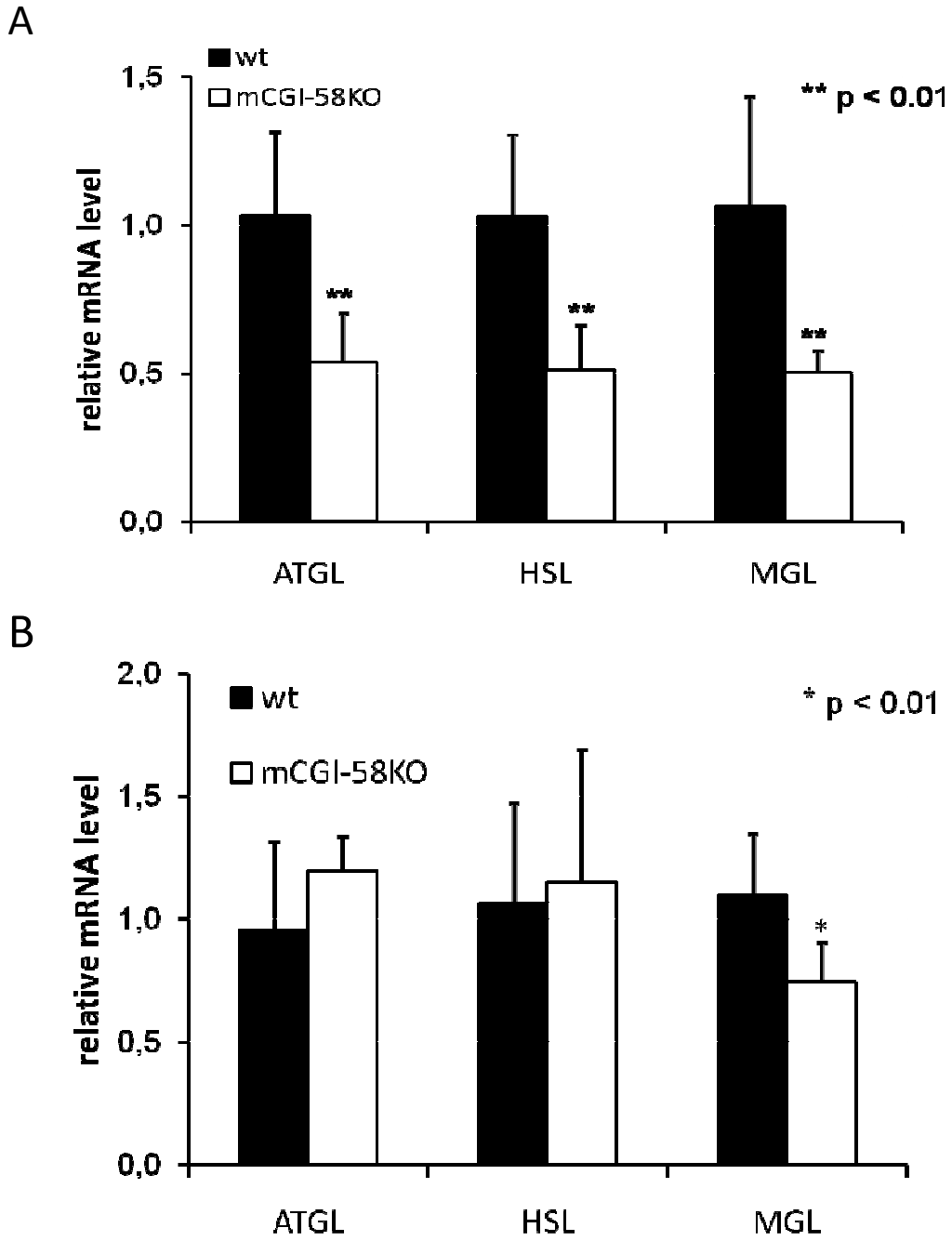

Figure 4.1.2 **relative mRNA levels of cellular lipases are reduced in cardiac but not skeletal mCGI-58KO muscle** (A) relative lipase mRNA levels of ATGL, HSL and MGL in cardiac muscle of wt and mCGI-58KO mice (n = 6) (B) relative lipase mRNA levels of ATGL, HSL and MGL in skeletal muscle of wt and

mCGI-58KO mice (n = 5). The relative mRNA levels were determined by qRT-PCR. Data are shown as mean ± SD. *P < 0.05, **P < 0.01 and ***P < 0.001 versus wt mice.

Accordingly, the observed increase in ATGL protein levels in CM and SM of mCGI-58KO mice does not result from increased in mRNA expression. Furthermore, mRNA levels of other lipases (HSL and MGL) were also decreased in these mice. Taken together, these findings indicate that the increase in ATGL protein levels in CM of CGI-58KOM mice involve post-translational mechanisms. We further asked us, if the observed accumulation of ATGL protein is a general response to the lipolytic defect and ectopic lipid accumulation or unique to CGI-58 deficiency. Therefore, we investigated protein expression levels of genes implicated in lipolysis in ATGL-deficient (ATGL-KO) mice which show massive cardiac steatosis.

4.2 CGI-58 is increased in ATGL-deficient CM

To examine whether ATGL protein accumulation is unique for CGI-58 deficiency or a common response to a defect in lipolysis, we measured CGI-58 protein expression levels via Western Blotting of CMhomogenates prepared from ATGL-KOmice and controls, respectively.

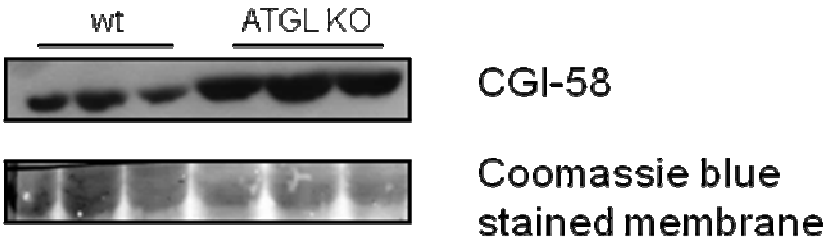

Figure 4.2 **CGI-58 protein levels are increased in ATGL-deficient (ATGL-KO) CM**. Western Blot analysis of CGI-58 protein levels in ATGL deficient CM (30 µg) compared to levels of controls (ATGL flox/flox mice). The blotting membrane was stained with Coomassie blue to check for even protein loading. CGI-58 has a molecular weight of 37kDa.

ATGL KO mice show a marked increase (5-fold) in CGI-58 protein levels compared to wt (figure 4.2) in analogy to increased ATGL protein levels found in CM of mCGI-58KO mice. This similar response in both models of cardiac steatosis provides further evidence for the existence of post-translational mechanism(s) attempting to restore lipolytic function. However, if CGI-58 accumulation in ATGL-KO CM underlies the same

or a divergent mechanism demands further clarification. This prompted us to examine if CGI-58 knockdown similarly affect ATGL protein levels in a cell culture approach.

4.3 CGI-58 does not influence ATGL protein levels *in vitro*

In order to elucidate if CGI-58 protein expression (or its knock down) directly influences ATGL protein expression levels, a cell culture system using H9C2 cells [98] was established. The myocytes were differentiated according to an adjusted in-house protocol to assume cardiomyocyte-like features. Differentiated H9C2 cells are often used as cardiomyocyte cell culture model for inhibitor studies to minimize biochemical and substrate alterations. In our approach, differentiated H9C2 myocytes were infected with an adenovirus construct carrying plasmids for lacZ and CGI-58 overexpression.

Different multiplicity of infection (MOI) levels were used to generate increasing amounts of CGI-58 protein expression to investigate a potential correlation among CGI-58 and ATGL protein expression levels. However, different CGI-58 expression levels in H9C2 myocytes did not influence ATGL protein levels. This finding suggests that CGI-58 itself does not affect ATGL protein expression.

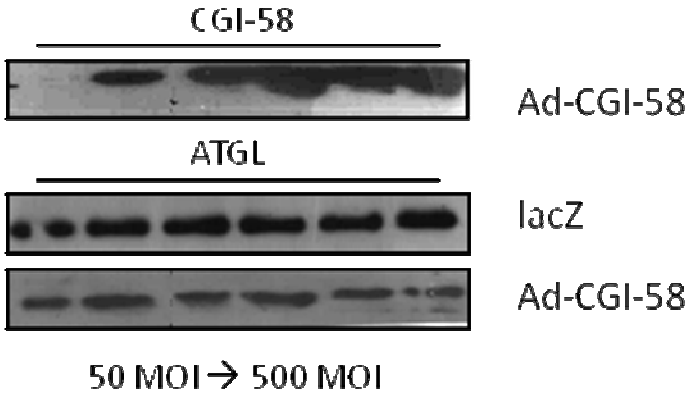

Figure 4.3 **CGI-58 overexpression does not directly influence ATGL protein levels**. Differentiated H9C2 myocytes were infected with different MOI of adenoviruses encoding CGI-58 or lacZ (control). CGI-58 overexpression was confirmed (upper panel) and ATGL expression pattern was compared to lacZ (lower panel) using Western Blot analysis. (MOI, multiplicity of infection)

4.4 Examination of ATGL protein stability

4.4.1 ATGL half-life is influenced by the proteasome specific inhibitor MG132

To address ATGL protein turn over, H9C2 cells were treated with cycloheximide (CHX), an inhibitor of protein *de novo* biogenesis, and harvested at various time points after incubation. It has been suggested that ATGL is a rather short-lived protein with a half-life of about 45 minutes in hamster embryonic kidney-293 (HEK293) cells [99]. However in our H9C2 myocyte system, ATGL is still detectable after 24 h (figure 4.4.1). This divergence is possibly accounted for by the much lower proliferation rate of differentiated H9C2 myocytes compared to HEK293. Nevertheless, we found that protein degradation could be attenuated by addition of the proteasome-specific inhibitor MG132. In contrast, lysosomal or general protease inhibitors showed no effect on ATGL protein stability (figure 4.4.1).

Until now, we were unable to provide physical evidence of ATGL ubiquitination, and no report regarding ATGL ubiquitination could be found in the literature. Therefore, it is unclear, how the proteasome mechanistically affects ATGL protein stability.

However, as many heart diseases are associated with proteasome dysfunction [100], this finding possibly provides an interesting link between the ubiquitin-proteasome system and the regulation of lipolysis.

A

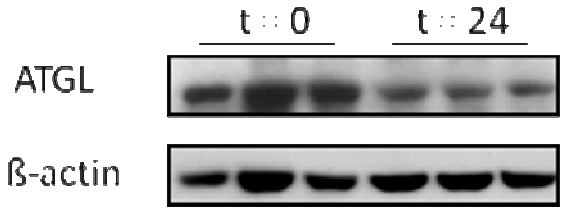

B

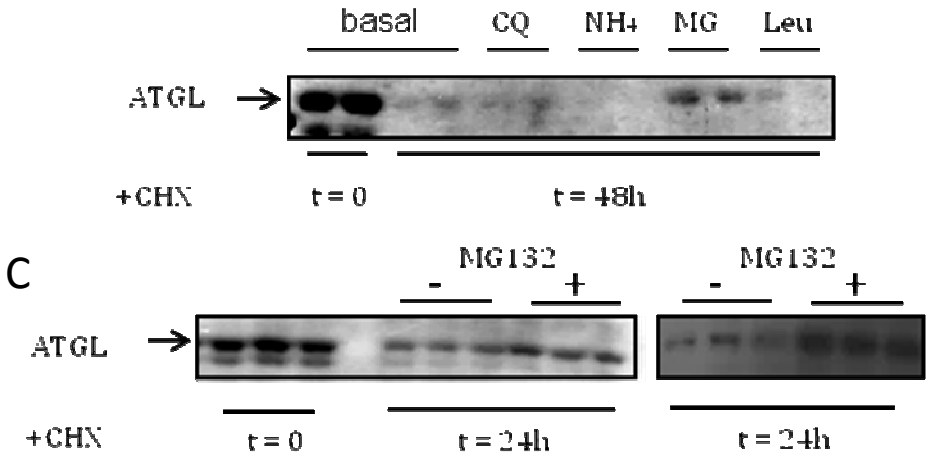

Figure 4.4.1 **ATGL protein levels are affected by the ubiquitin-proteasome system** (A). ATGL half-life was estimated using Western Blot analysis after harvesting cells at different time points following CHX treatment. (B, C) ATGL degradation is dependent on proteasome activity. Differentiated H9C2 were treated with CHX, then leupeptin (an inhibitor of trypsin and cysteineproteases), or NH_4Cl /Chloroquine (both general lysosomal protease inhibitors), or MG132 (a proteasome-specific inhibitor**)** were added to the culture medium. ATGL protein level was evaluated using Western Blotting. (CQ, Chloroquine [50 µM]; NH_4Cl [10 µM]; MG, Mg132 [10 µM]; Leu, Leupeptine [10 µM]).

4.4.2 ATGL protein abundance correlates with AMPK activation and inhibition

The role of AMPK in lipolysis has been very controversial, with data reporting induction [101], inhibition [102] or no effect [103] on lipolysis. Investigation of ATGL mRNA levels only showed small effects in differentiated H9C2 myocytes upon AMPK stimulation or inhibition with5-aminoimidazole-4-carboxamide ribonucleotid (AICAR) or Compound C (CC), respectively. AICAR induced activation of AMPK showed a minor increase (+ 22 %) in ATGL mRNA expression compared to non-stimulated control. Controversially, CC-mediated AMPK inhibition further increased (+ 58%) ATGL mRNA expression compared to control in differentiated H9C2 myocytes (figure 4.4.2).

However and interestingly, ATGL protein levels increased in differentiated H9C2 cardiomyocytes upon AMPK activation (2-fold). In accordance with our findings, others have also reported ATGL accumulation upon AICAR stimulation in AT [96], however the mechanism for this accumulation was not addressed. More intriguingly, AMPK inhibition mediatedby CC drastically reduced ATGL protein levels (- 95 %) compared to controldespite enhanced ATGL mRNA expression. This discrepancy in

ATGL mRNA expression and protein abundance argue for a role of AMPK in regulating ATGL in a transcription-independent manner.

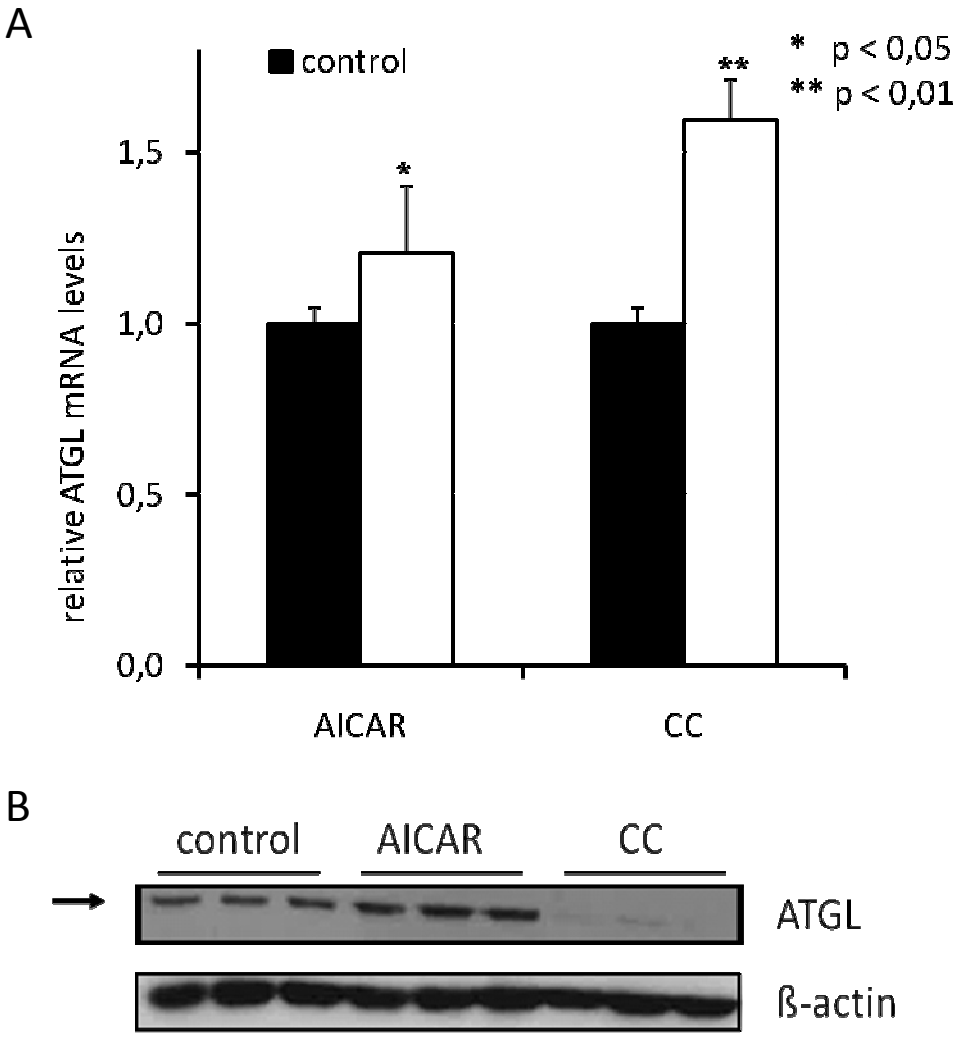

Figure 4.4.2 **AMPK affects ATGL mRNA and protein protein expression.** (A) ATGL mRNA and (B) protein levels upon AMPK stimulation (AICAR incubation) and inhibition (CC incubation) in differentiated H9C2 myocytes. Non-stimulated H9C2 myocytes were used as control. The relative ATGL mRNA levels were determined by qRT-PCR and protein levels were determined by Western blot. ß-actin was used as house keeping gene. Data are shown as mean ± SD. *P < 0.05, **P < 0.01 and ***P < 0.001 vs. control. AICAR… 5-aminoimidazole-4-carboxamide ribonucleotid, CC… Compound C

4.5 AMPK activation increases TG catabolism

AMPK has been reported to be able to phosphorylate ATGL at serine 406 [9]. Therefore, we created serine406 -> alanine / aspartic acid ATGL mutants (hereafter referred as S406A and S406D respectively) to investigate effects of S406 phosphorylation on ATGL hydrolytic activity.S406A serves as a model of a

constitutively “non-phosphorylated” ATGL, and S406D as constitutively “phosphorylated” ATGL, respectively. We hypothesized that phosphorylation at S406, which constitutes a canonical 14-3-3 binding motif, might induce ATGL localization to the LD surface and thereby increasing lipolytic activity. In contrast, S406A should not be recruited to LD via AMPK stimulation. However, it is very likely, that there are also other mechanisms involved in regulating ATGL localization, so we still expect some ATGL activity and localization at the LD surface.

To estimate the impact of AMPK on TG catabolism, COS-7 cells were transfected with ATGL, lacZ and S406A and loaded with oleic acid for 20h to induce TG incorporation. In parallel to oleic acid loading, ATGL transfections were also treated with AICAR and CC. As expected, cells expressing recombinant ATGL show reduced TG content (- 80 %), which could be even further reduced with AICAR stimulation (figure 4.5). In contrast, inhibition of AMPK with CC only reduced TG content by 50% compared to the lacZ expressing control. Intriguingly, TG content in COS-7 cells transfected with recombinant S406A was only slightly reduced (- 15 %) compared to control.

It has been suggested that S406 phosphorylation enhances the catalytic activity of ATGL [95]. However, we assumed that ATGL hydrolytic activity *in vitro* is unchanged in S406A or S406D mutated ATGL compared to wt ATGL. Presumably, the observed differences in hydrolytic activity result from differences in ATGL protein concentrations affected by the mutations, which could by a direct result of altered ATGL protein stability. Therefore, we checked ATGL protein abundance in the lysates used for the TG hydrolytic assay with Western blot analysis. As expected, ATGL protein levels are significantly altered in S406A (- 50%) compared to ATGL and S406D (figure 4.5), what corresponded directly to the observed decrease of hydrolytic activity *in vitro*. Accordingly, we conclude that AMPK mediated phosphorylation of S406 increases the hydrolytic activity of ATGL by promoting the stabilization of the lipase rather than its catalytic activity.

A

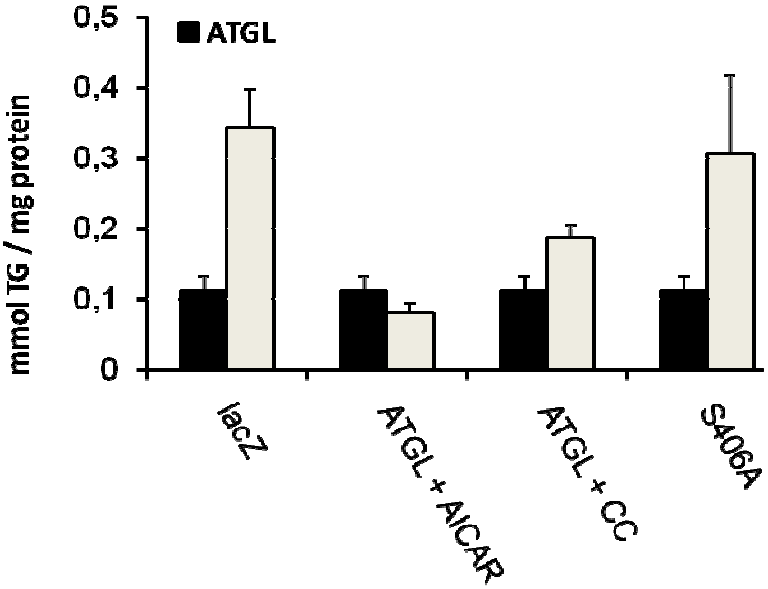

B

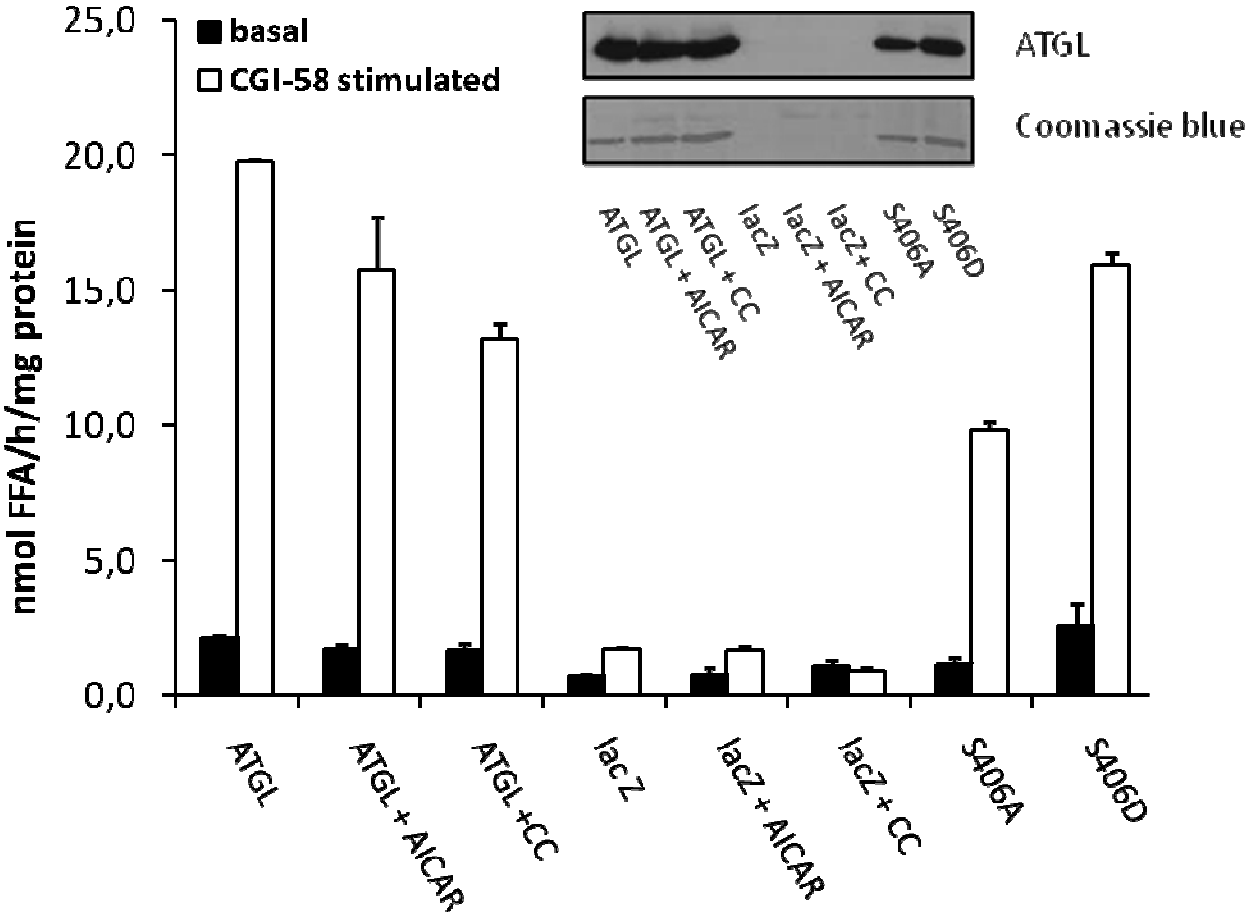

Figure 4.5 **S406 phosphorylation affects ATGL-mediated TG catabolism *in vivo* in contrast to unchanged *in vitro* ATGL TG hydrolytic activity.** (A) TG content in COS-7 cells after transfection with ATGL, lacZ and S406A and subsequent loading with oleic acid for 20 h. (B) TG hydrolytic activity of S406A/D and ATGL compared lacZ under basal, AMPK stimulated and AMPK inhibited conditions. 50 µg protein from COS7-cell lysates was used for TG-hydrolytic assay and 30 µg protein was loaded onto the gel for Western Blot expression analysis. TG hydrolytic activities were measured by using ^{3}H-labeled Triolein as substrate. AICAR, 5-aminoimidazole-4-carboxamide ribonucleotid; CC, Compound C; FFA, free fatty acid; TG, triglycerides.

4.6 Cardiac ATGL turnover and proteasome activity

Recently, the study by Pollak *et al.* from our laboratory showed that cardiac specific Perlipin-5 over-expression in CM provokes severe cardiac steatosis [10] as a consequence of a barrier established by Perilipin-5 that shields LD TG against hydrolysis from cellular lipases. With respect to the impact of muscle CGI-58 deficiency on cardiac lipolysis and ATGL protein levels we hypothesized that ATGL protein levels may be also increased in Plin5 overexpressing mice in response to impaired lipolysis. Therefore, we investigated ATGL protein expression in CM of perilipin-5 (CM-Plin5) over-expressing mice with Western blot analysis (figure 4.6). As hypothesized, ATGL protein content was markedly increased in CM-Plin5 transgenic mice, and a similar increase was also found for its co-activator CGI-58 [10].

The diseased heart shows numerous metabolic changes and many proteinopathies are associated with cardiac disease. Therefore, we investigated proteasome function to examine whether changes in ATGL/CGI-58 protein levels are the consequence of a global defect in proteasome activity caused by cardiac steatosis. Proteasome chemotryptic activity was measured by fluorescence spectrometry of crude cytosol preparations from CM incubated with a peptide-linked fluorophore. Upon peptide degradation by the proteasome, the fluorophore is cleaved and released resulting in an increase in fluorescence intensity whichis directly proportional to proteasome activity. Unexpectedly, we observed an increase (+ 33 %) in proteasome chymotryptic activity from CM-Plin5 and wt cardiac muscle (figure 4.6). Therefore, we conclude that it is unlikely that the increase in ATGL and CGI-58 levels is due to impaired proteasomal activity in CM of CM-Plin5 transgenic mice. The increased chymotryptic activity found in steatotic CM of CM-Plin5 transgenic mice prompted us to check proteasome activity in other steatotic tissues. However, chymotryptic activity in steatotic liver samples of mice lacking CGI-58 exclusively in the liver (CGI-58livKO) was unchanged compared to CGI-58 flox/flox mice. Therefore we conclude that the observed increase of proteasome chymotryptic activity is specific to CM, which is in line with other observations comparing liver and heart proteasome function [9].

However, if and to which extend this increase in chymotryptic activity has an influence ATGL protein level or turnover remains to be further investigated. In summary, our data indicate that the proteasome might be influenced by TG turnover in CM, at least in the pathological system of cardiac steatosis.

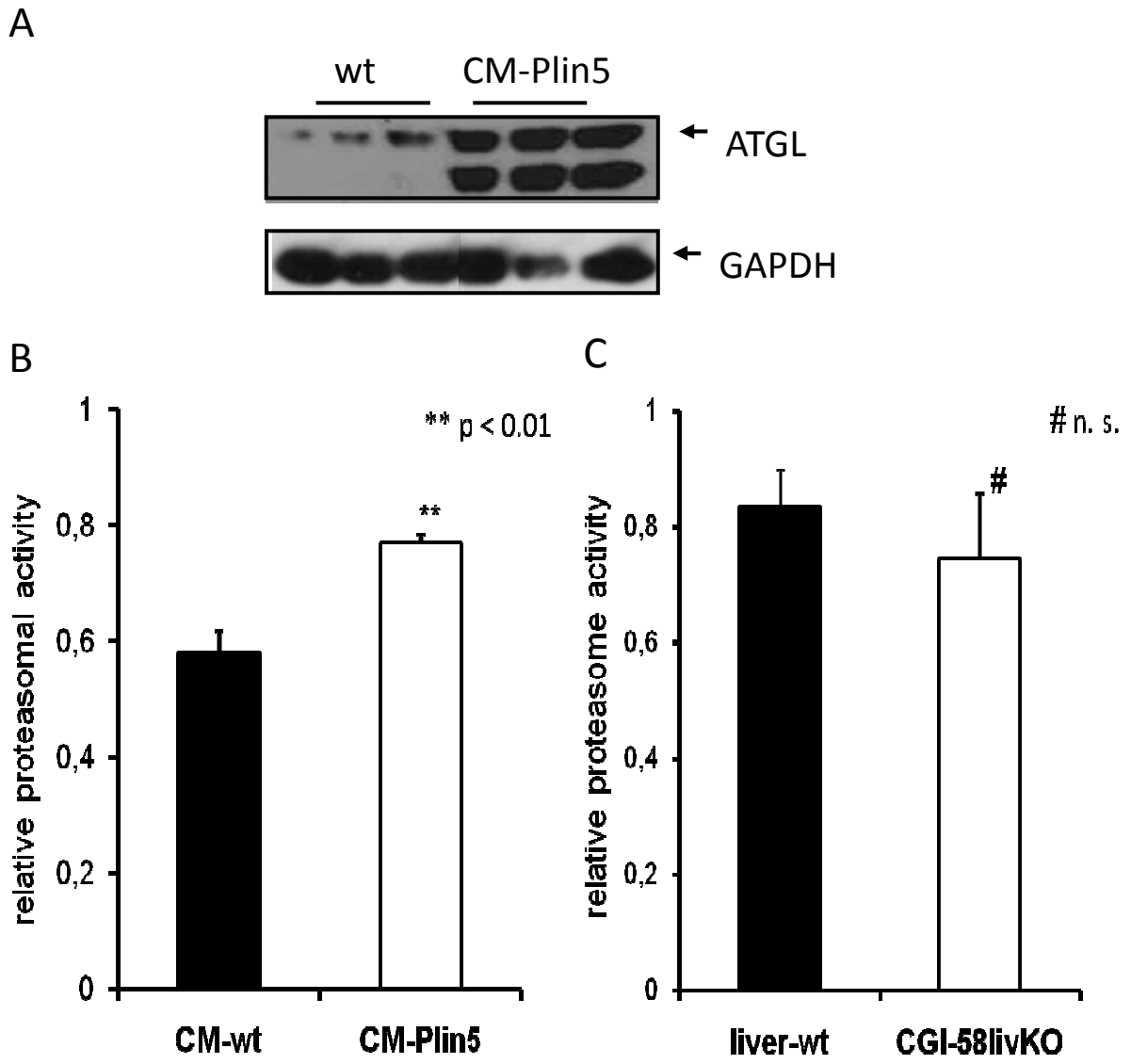

Figure 4.6 **CM-specific Plin5 overexpression affects ATGL protein levels and proteasome chymotryptic activity** (A) Protein expression levels of ATGL were markedly elevated in CM of CM-Plin5 mice compared with wt. Analyzed samples contained 30 µg protein. GAPDH was used as a house keeping gene. (B) Proteasome chymotryptic activity is enhanced in steatotic CM-Plin5 samples compared to wt (n = 3). (C) Proteasome chymotryptic activity is not effected in steatotic liver samples of mice lacking CGI-58 exclusively in the liver (CGI-58livKO) compared to wt (n = 6). Chymotryptic activity was measured using a fluorogenic peptide. Data are shown as mean ± SD. # not significant P > 0.05, *P < 0.05, **P < 0.01 and ***P < 0.001 versus wt mice.

5) Discussion

The last decade delivered major insights into the lipolytic process of TG mobilization in AT. However, lipolysis in non-adipose tissues is much less understood and awaits further examination. The generation and characterization of lipase-deficient mouse models shed new light in the molecular mechanism of TG catabolism in non-adipose tissue and these animal models did not only harbor changes in body fat mass but also suffered from a variety of obesity related co-morbidities including renal and cardiac dysfunction and skin barrier defects. Today, there is overwhelming evidence that functional lipolysis is critical for normal liver and heart function as well for lipid metabolism and signaling in many other organs including the brain and skin.

In the heart, defects in lipolysishave a strong impact on cardiac energy homeostasis, leading to severe steatosis and lethal cardiac dysfunction. Interestingly, we found that cardiac steatotic ATGL and CGI-58 deficient, as well as Plin-5 over-expressing transgenic mice, share common properties. For example, these mice exhibit ectopic lipid accumulation, reduced TG hydrolytic activities, impaired mitochondrial function anda switch in substrate utilization from FA to carbohydrates. Moreover, there are not only morphologic similarities like cardiac fat accumulation, but also in the adaptive response to the lipolytic defect. Representatively, ATGL-KO mice exhibit elevated CGI-58 protein levels and inversely, mCGI-58KO mice show elevated ATGL protein levels, whereas CM-Plin5 mice accumulate both, ATGL and CGI-58 protein.As these changes on the protein levels are not paralleled by changes in mRNA levels of these genes we hypothesized that post-translational modificationsmay causative for the elevated protein levels. We also showed *in vitro*, that ATGL protein levels are not influenced directly by CGI-58 protein abundance. Within this context, we assumed that there may exist a common regulatory pathway, which senses the energy imbalance caused by impaired TG catabolism and attempts to restore lipolysis via protein stabilization. In accordance with this hypothesis, the compensatory increase of ATGL protein level observed in mCGI-58KO CM may also explain differences in the clinical picture caused ATGL or CGI-58 deficiency, as solely ATGL-deficiency is causative for massive cardiac

steatosis and in some cases lethal heart dysfunction. However, the compensatory increase of ATGL protein in mCGI-58KO CM is not sufficient to prevent the development of cardiac steatosis caused by CGI-58 deficiency and impaired lipolysis. Surprisingly, mCGI-58KO skeletal muscle is less affected by CGI-58 deficiency, suggesting that the observed increase in ATGL protein is able to compensate for lipolytic defect in SM, at least to a certain extent [97]. Differences in cardiac and skeletal muscle pathogenesis might also arise from substrate utilization, with SM taking up 60-90 % of glucose from the circulation; while the healthy adult heart relies to a large extent on fatty acid oxidation.

In this study, potential pathways were examined that could be involved in the posttranslational regulation of ATGL and its consequences for TG hydrolysis and energy metabolism.

(1) ATGL protein degradation is mediated by the ubiquitin-proteasome system (UPS). In a cycloheximide-based protein degradation experiment, we and others have found that ATGL degradation can be attenuated by addition of a proteasome-specific inhibitor whereas lysosomal degradation or protease inhibitors showed no effect on ATGL protein turn over. However, a drawback of this study is the lack of data confirming that ATGL is indeed ubiquitinated, a prerequisite for proteasome-mediated protein turn over. Furthermore, neither data regarding ATGL ubiquitination or its association with known E3-ligases have been reported so far. It remains to be clarified how the proteasome interferes with ATGL protein homeostasis. Cellular stress like hypoxia or oxidative stress may lead to the activation of the ubiquitine proteasome system (UPS). The UPS is a highly and dynamically regulated system, integrating signal input from many external and internal events. Accordingly, the UPS has been linked to many forms of cardiac disease [100]. As defects in lipolysis are associated with altered energy metabolism and mitochondrial dysfunction, it is reasonable to assume altered proteasome activity/function in our mouse models harboring cardiac steatosis. Arguably, impaired mitochondrial function caused by loss of CGI-58 or ATGL or

overexpression of Plin-5 may lead to reduced ATP production, activating energy producing and expenditure conserving pathways. However, the role of the proteasome in responding to cellular stress has been controversial. For example, proteasome activity has been shown to be activated during starvation [108], sepsis [109], severe trauma [110] and cancer cachexia [111], whereas proteasome hyperactivation in the heart protects against cardiac proteinopathy and myocardial ischemia-reperfusion injury [112].Interestingly, we found that proteasome chymotryptic activity is enhanced in CM preparations of CM-Plin5 mice showing cardiac steatosis compared to wt cardiac preparations. Furthermore, we showed that this increase in proteasome activity is unique for cardiac steatosis, while proteasome activity in steatotic liver samples was unchanged. Comparison of proteasomes from liver and hearts has been shown that the liver carries significantly higher amounts of phosphorylated proteins and is less sensitive to proteasome inhibitors, possibly accounting for this difference [110]. Activation of the UPS has been described in different models of cardiac hypertrophy; however the role of the proteasome in response to steatosis induced by dysfunctional lipolysis is quite unclear. Nevertheless, there is one study reporting an increase in proteasome activity in streptozotocin-induced diabetic rats, a model of experimental hyperglycemia [113]. They showed that proteasome non-ATP-dependent chymotryptic activity was increased over 2-fold in hyperglycemic hearts, but the ATP-dependent activity was decreased and levels of ubiquitinated proteins were increased. Arguably, ATP deficiency reduces tryptic- and peptidyl-glutamyl peptide-hydrolyzing **(**PGPH)-like activities but promotes chymotryptic activity not only in hyperglycemia, but in other forms of energy-related metabolic diseases. Related to this finding, it is allowed to assume that ATP-producing pathways, including lipolysis, are severely affected by altered proteasome activities. It is even conceivable that enhanced proteasome activity is a means to improve TG catabolism by reducing the substrate “shielding” function of perilipins against cellular lipases, because many LD associated coating proteins are shown to be rapidly degraded by the proteasome [78-81].

(2) When considering energy imbalance, the ancient ATP-sensor AMPK has to be discussed as well. The role of AMPK in lipolysis has been very controversial, with data reporting induction [101], inhibition [102] or no effect [103] on lipolysis.We found that AMPK has significant effects on ATGL protein abundance; activation of AMPK promotes ATGL accumulation, whereas inhibition of AMPK markedly reduces ATGL protein levels. As neither one of these effects corresponded with the transcriptional output, we assumed that AMPK directly interacts with ATGL, rather than initiating a transcriptional program. Supporting this assumption, others have reported that S406 and S430 of ATGL can be phosphorylated by AMPK, constituting a 14-3-3 binding motif [95].

Investigation of S406A and S406D mutants further support the role of AMPK in regulating TG catabolism via ATGL, although it is yet unclear if S406 phosphorylation induces TG catabolism by a change in ATGL localization, stability or even conformation and/or catalytic function. However, we found that ATGL hydrolytic activity *in vitro* is independent of S406 phosphorylation, strongly suggesting that the observed increase in TG catabolism*in vivo* is a result of improved ATGL protein stability or abundance at the lipid droplet. In line with our findings, it has been proposed that S406 phosphorylation induces binding to LD-associated proteins via its 14-3-3 binding motif [114]. Furthermore, it was shown that S406A is less abundantly localized to the LD compared to wt ATGL at least in COS-7 cells [114]. Accordingly, it is tempting to speculate that AMPK phosphorylation is a mechanism which facilitates ATGL translocation to LD similar to PKA-mediated HSL translocation. Additionally, we assume that ATGL translocation and 14-3-3 binding might be responsible for increased protein stability observed upon AICAR stimulation. Correspondingly, AMPK inhibition with CC disrupts 14-3-3 binding thereby facilitating its degradation. If S406 de-phosphorylation is required for ATGL degradation is not known, and a phosphatase that specifically dephosphorylates ATGL has not been discovered so far. However, we assume that the unphosphorylated state of S406 subjects ATGL to ubiquitination and proteasome degradation. This is an important challenge for ongoing experiments to unravel the role of the UPS in the regulation of ATGL protein level. Finally, it is also

conceivable that the observed effects of AMPK on TG catabolism are not exclusively mediated by ATGL, since AMPK is involved in many, mostly redundant, signaling processes.

In summary, the following scenario is assumable. In the basal energy state, ATGL is a relatively short-lived protein and ATGL that is localized in the cytosol is subjected to proteasomal degradation. Upon energy demand, ATGL is further recruited to the LD surface, where it interacts with LD associated proteins. This facilitated translocation of ATGL enhances TG hydrolysis by improving ATGL abundance and substrate accessibility at the LD surface.

Given that the energy requirements of cardiomyocytes cannot be fulfilled, a whole cascade of compensatory mechanisms is activated in response to falling ATP levels. These include reduction in tryptic- and PGPH-like proteasome activity and activation of ATP-independent chymotryptic activity. Additionally, the ATP-sensor AMPK is activated, initiating a multitude of energy producing and preserving pathways. With regard to lipolysis, we suggest that AMPK and the UPS are critically involved in TG catabolism by direct interaction with and in regulating ATGL protein abundance. To elucidate the molecular mechanisms causing increased ATGL protein levels in the diseased heart may deliver therapeutic targets to interfere with the development of cardiac disorders including cardiomyopathy.

6) Abbreviations

ADRP	adipose differentiation-related protein
AMPK	5-AMP activated protein kinase
ATGL	adipose tissue triglyceride lipase
ATP	adenosine-5'-triphosphate
BAT	brown adipose tissue
BCA	bicinchoninic acid
BMI	Body Mass Index
BSA	bovine serum albumin
cAMP	cyclic adenosine monophosphate
CAPS	N-cyclohexyl-3-aminopropanesulfonic acid
CDC	Center for Disease Control and Prevention
cDNA	complementary DNA
CDS	ChanarinDorfman Syndrome
CE	cholesteryl ester
CGI-58	comparative gene identification-58
CGI-58f/f wt	CGI-58 “floxed” wild type
CM	cardiac muscle
DEPC	diethylpyrocarbonate
DG	diacylglycerol
DTT	dithiothreitol
EDTA	ethylene diamine tetra-aceticacid
FA	fatty acid
FFA	free fatty acid
G0S2	G_0/G_1 switch gene 2
HSL	hormone-sensitive lipase
kDa	kilodalton
KO	knock-out
LD	lipid droplet
livCGI-58KO	liver-specific CGI-58 knock-out
MG	monoacylglycerol

MGL	monoglyceride lipase
MLDP	myocardial lipid droplet binding protein
MOPS	3-(N-morpholino)propanesulfonic acid
mRNA	messenger RNA
NLSD	neutral lipid storage disease
NLSDI	NLSD with ichthyosis
PCR	polymerase chain reaction
PKA	protein kinase A
PVDF	polyvinyliden fluoride
RNA	ribonucleic acid
SDS	sodium dodecyl sulfate
SDS-Page	sodium dodecyl sulfate polyacrylamide gel electrophoresis
SM	skeletal muscle
TEMED	tetra methyl ethylene diamine
TG	triglyceride
TGH	triglyceride hydrolase
UPS	ubiquitin-proteasome system
WAT	white adipose tissue
WHO	World Health Organization
Wt	wild type

6) References

[1] WHO Obesity: preventing and managing the global epidemic. WHO Technical Report Series number 894WHO, Geneva (2000)

[2] WPT James, R Jackson-Leach, C Ni Mhurchu*et al.*Overweight and obesity (high body mass index)

[3] M Ezzati, AD Lopez, A Rodgers, CJL Murray (Eds.), Comparative quantification of health risks: global and regional burden of disease attributable to selected major risk factors, vol. 1 WHO, Geneva (2004), pp. 497–596

[4] M Ezzati, AD Lopez, A Rodgers, S Vander Hoorn, CJ Murray. Comparative Risk Assessment Collaborating Group, Selected major risk factors and global and regional burden of disease Lancet, 360 (2002), pp. 1347–1360

[5] CDC (Center for Disease Control and Prevention) http://www.cdc.gov/obesity/defining.html [03.01.2013]

[6] KG Alberti, PZ Zimmet. Definition, diagnosis and classification of diabetes mellitus and its complication, part 1: diagnosis and classification of diabetes mellitus, provisional report of a WHO consultation Diabetic Med, 15 (1998), pp. 539–553

[7] MH Kim, MK Kim, BY Choi, YJ Shin. Prevalence of the metabolic syndrome and its association with cardiovascular diseases in Korea. J Korean Med Sci, 19 (2004), pp. 195–201

[8] WHO (World Health Organization): http://www.who.int/topics/obesity/en/ 03.01.2013

[9] W. B. Kannel, Vital epidemiologic clues in heart failure. J. Clin. Epidemiol.53, 229–235 (2000).

[10] Unger, R. H. (2003). Minireview: weapons of lean body mass destruction: the role of ectopic lipids in the metabolic syndrome. Endocrinology, 144(12) 5159–5165

[11] Montani, J-P; Carroll, J. F.; Dwyer, T. M.; Antic, V.; Yang, Z.; Dulloo, A. G. (2004). Ectopic fat storage in heart, blood vessels and kidneys in the pathogenesis of cardiovascular diseases. International journal of obesity and related metabolic disorders 28(4) S58-65.

[12] Nelson D., Cox L. (2004). Lehninger Principles of Biochemistry, 4th Edition. W.H. Freeman and Co. New York. p. 343-348, 631-637, 690-722.

[13] Heineke J.;Molkentin J.D. (2006) Regulation of cardiac hypertrophy by intracellular signalling pathways Nature Reviews Molecular Cell Biology 7, 589-600 (August 2006) | doi:10.1038/nrm1983

[14] Frey N, Luedde M, Katus HA (2011) Mechanisms of disease: hypertrophic cardiomyopathy.Nat Rev Cardiol. 2011 Oct25;9(2):91100.doi:10.1038/ nrcardio.2011.159.

[15] Mantena, S. K.; King, A. L.; Andringa, K. K.; Eccleston, H. B.; Bailey, S. M. (2008). Mitochondrial dysfunction and oxidative stress in the pathogenesis of alcohol- and obesity-induced fatty liver diseases. Free radical biology & medicine, 44(7) 1259–1272

[16] Young SG &Zechner R; Biochemistry and pathophysiologyof intravascular and intracellular lipolysis. Access the most recent version at doi: 10.1101/gad.209296.112 Genes Dev. 2013 27: 459-484
[17] Glatz JFC, Luiken JJFP, Bonen A. Membrane Fatty Acid Transporters as Regulators of Lipid Metabolism: Implications for Metabolic Disease Physiol Rev90: 367– 417, 2010; doi:10.1152/physrev.00003.2009.
[18] Duncan RE, Ahmadian M, Jaworski K, Sarkadi-Nagy E, Sul HS. Regulation oflipolysis in adipocytes.Annu Rev Nutr 2007;27:79–101.
[19] Langin D. Control of fatty acid and glycerol release in adipose tissue lipolysis.
CR Biol 2006;329:598–607 [discussion 653–655].
[20] Zechner R, Strauss JG, Haemmerle G, Lass A, Zimmermann R. Lipolysis:pathway under construction. CurrOpinLipidol 2005;16:333–40
[21] Brasaemle, Dawn L.; Dolios, Georgia; Shapiro, Lawrence; Wang, Rong (2004). Proteomic analysis of proteins associated with lipid droplets of basal and lipolytically stimulated 3T3-L1 adipocytes. The Journal of biological chemistry, 279(45) 46835–46842.
[22] Brasaemle, D. L. (2007) J. Lipid Res. 48, 2547–2559
[23] Wolins, N. E., Brasaemle, D. L., and Bickel, P. E. (2006) FEBS Lett. 580, 5484–5491
[24]Wang, H. et al (2011) Unique regulation of adipose triglyceride lipase (ATGL) by perilipin 5, a lipid droplet-associated protein. J. Biol. Chem. 28:15707 – 15715
[25] Pollak NM M. Schweiger, D. Jaeger, D. Kolb, M. Kumari, R. Schreiber, S. Kolleritsch, P. Markolin, G. F. Grabner, C. Heier, K. A. Zierler, T. Rülicke, R. Zimmermann, A. Lass, R. Zechner, and G. Haemmerle(2013) Cardiac-specific overexpression of perilipin 5 provokes severe cardiac steatosis via the formation of a lipolytic barrier. J Lipid Res. 2013 Apr;54(4):1092-102. doi: 10.1194/jlr.M034710. Epub 2013 Jan 23.
[26] Fujimoto, T., and Parton, R. G. (2011) Not just fat: The structure and function of the lipid droplet. Cold Spring Harb.Perspect.Biol.3, a004838.
[27] Brasaemle, D. L., and Wolins, N. E. (2012) Packaging of fat: an evolving model of lipid droplet assembly and expansion. J Biol Chem287, 2273-2279
[28] Lass A., R. Zimmermann, M. Oberer, and R. Zechner (2011) Lipolysis - a highly regulated multi-enzyme complex mediates the catabolism of cellular fat stores. Prog. Lipid Res. 50 : 14 – 27
[29] Zimmermann, R.; Strauss, J. G.; Haemmerle, G.; Schoiswohl, G.; Birner-Gruenberger, R.; Riederer, M. et al. (2004). Fat mobilization in adipose tissue is promoted by adipose triglyceride lipase. Science (New York, N.Y.), 306(5700) 1386
[30]Lass A., R. Zimmermann, G. Haemmerle, M. Riederer, G. Schoiswohl, M. Schweiger, P. Kienesberger, J. G. Strauss, G. Gorkiewiczand R. Zechner(2006) Adipose triglyceride lipase - mediated lipolysis of cellular fat stores is activated by CGI-58 and defective in Chanarin-Dorfman syndrome. Cell Metab.3 : 309 – 319
[31] Duncan RE, Wang Y, Ahmadian M, Lu J, Sarkadi-Nagy E, Sul HS. Characterization of desnutrin functional domains: critical residues for triacylglycerol hydrolysis in cultured cells. J Lipid Res 2010;51:309–17
[32] Schweiger M., M. Paar , C. Eder, J. Brandis, E. Moser, G. Gorkiewicz , S. Grond, F. P. Radner , I. Cerk, I. Cornaciu et al. (2012) G0/G1 switch gene-2 regulates human

adipocyte lipolysis by affecting activity and localization of adipose triglyceride lipase. J. Lipid Res. 53 : 2307 – 2317
[33] Schweiger, M., Schoiswohl, G., Lass, A., Radner, F.P., Haemmerle, G., Malli, R., Graier, W., Cornaciu, I., Oberer, M., Salvayre, R., et al. (2008). The C-terminal region of human adipose triglyceride lipase affects enzyme activity and lipid droplet binding. J. Biol. Chem. 283, 17211–17220.
[34] Haemmerle G., A. Lass, R. Zimmermann, G. Gorkiewicz, C. Meyer , J. Rozman, G. Heldmaier, R. Maier, C. Theussl, S. Eder, et al. (2006) Defective lipolysis and altered energy metabolism in mice lacking adipose triglyceride lipase. Science 312: 734 - 737
[35] Haemmerle G., T. Moustafa, G. Woelkart, S. Buttner , A. Schmidt , T. van de Weijer, M. Hesselink, D. Jaeger, P. C. Kienesberger , K. Zierler et al (2011) ATGL-mediated fat catabolism regulates cardiac mitochondrial function via PPAR-alpha and PGC-1. Nat. Med. 17 : 1076 – 1085
[36] Fischer, J., Lefevre, C., Morava, E., Mussini, J. M., Laforet, P., Negre-Salvayre, A., Lathrop, M., and Salvayre, R. (2007) Nat Genet 39, 28-30
[37] Ghosh, A.K., Ramakrishnan, G., and Rajasekharan, R. (2008). YLR099C (ICT1) encodes a soluble Acyl-CoA-dependent lysophosphatidic acid acyltransferase responsible for enhanced phospholipid synthesis on organic solvent stress in Saccharomyces cerevisiae. J. Biol. Chem. 283, 9768–9775
[38]Montero-Moran, G., Caviglia, J.M., McMahon, D., Rothenberg, A., Subramanian, V., Xu, Z., Lara-Gonzalez, S., Storch, J., Carman, G.M., and Brasaemle, D.L. (2010). CGI-58/ABHD5 is a coenzyme A-dependent lysophosphatidic acid acyltransferase. J. Lipid Res. 51, 709–719.]
[39] Gruber A, Cornaciu I, Lass A, Schweiger M, Poeschl M, Eder C, et al. The N-terminal region of comparative gene identification-58 (CGI-58) is important for lipid droplet binding and activation of adipose triglyceride lipase. J BiolChem 2010;285:12289–98
[40] Schweiger , M. , A. Lass , R. Zimmermann , T. O. Eichmann , and R. Zechner (2009) Neutral lipid storage disease: genetic disorders caused by mutations in adipose triglyceride lipase/PNPLA2 or CGI-58/ABHD5.Am. J. Physiol. Endocrinol. Metab. 297 : E 289 –E 296
[41] Radner F. P., I. E. Streith, G. Schoiswohl, M. Schweiger, M. Kumari, T. O. Eichmann, G. Rechberger, H. C. Koefeler, S. Eder, S. Schauer, et al. (2010) Growth retardation, impaired triacylglycerol catabolism, hepatic steatosis, and lethal skin barrier defect in mice lacking comparative gene identification-58 (CGI-58). J. Biol. Chem. 285 : 7300 – 7311
[42] Lefèvre, C., Jobard, F., Caux, F., Bouadjar, B., Karaduman, A., Heilig, R., Lakhdar, H., Wollenberg, A., Verret, J. L., Weissenbach, J., Ozguc, M., Lathrop, M., Prud'homme, J. F., and Fischer, J. (2001) Am J Hum Genet 69, 1002-12
[43] Radner, F. P., Streith, I. E., Schoiswohl, G., Schweiger, M., Kumari, M., Eichmann, T. O., Rechberger, G., Koefeler, H. C., Eder, S., Schauer, S., Theussl, H. C., Preiss-Landl, K., Lass, A., Zimmermann, R., Hoefler, G., Zechner, R., andHaemmerle, G. (2010) J BiolChem 285, 7300-11

[44] Lefevre, C., Jobard, F., Caux, F., Bouadjar, B., Karaduman, A., Heilig, R., Lakhdar, H., Wollenberg, A., Verret, J. L., Weissenbach, J., Ozguc, M., Lathrop, M., Prud'homme, J. F., and Fischer, J. (2001) Am. J. Hum. Genet. 69, 1002-1012
[45] Chanarin, I., Patel, A., Slavin, G., Wills, E. J., Andrews, T. M., and Stewart, G. (1975) Br. Med. J. 1, 553-555
[46] Yang X, Lu X, LombesM, Rha GB, Chi YI, Guerin TM, et al. The G(0)/G(1) switch gene 2 regulates adipose lipolysis through association with adipose triglyceride lipase. Cell Metab 2010;11:194–205
[47] Russell L, Forsdyke DR. A human putative lymphocyte G0/G1 switch gene containing a CpG-rich island encodes a small basic protein with the potential to be phosphorylated. DNA Cell Biol 1991;10:581–91
[48] Zandbergen F, Mandard S, Escher P, Tan NS, Patsouris D, Jatkoe T, et al. The G0/G1 switch gene 2 is a novel PPAR target gene. Biochem J 2005;392:313–24
[49] Yeaman, S. J. (1990). Hormone-sensitive lipase--a multipurpose enzyme in lipid metabolism. Biochimicaetbiophysicaacta, 1052(1) 128–132.
[50] Haemmerle, G.; Zimmermann, R.; Hayn, M.; Theussl, C.; Waeg, G.; Wagner, E. et al. (2002) Hormone-sensitive lipase deficiency in mice causes diglycerideaccumulation in adipose tissue, muscle, and testis. The Journal of biological chemistry, 277(7) 4806–4815
[51] Osterlund T, Danielsson B, Degerman E, Contreras JA, Edgren G, Davis RC, et al. Domain-structure analysis of recombinant rat hormone-sensitive lipase. Biochem J 1996;319(Pt 2):411–20.
[52] Harada, K.; Shen, W-J.; Patel, S.; Natu, V.; Wang, J.; Osuga, J. et al. (2003). Resistance to high-fat diet-induced obesity and altered expression of adipose specific genes in HSL-deficient mice. American journal of physiology. Endocrinology and metabolism, 285(6), 1182-95
[53] Tornqvist H, Belfrage P. Purification and some properties of a monoacylglycerol-hydrolyzing enzyme of rat adipose tissue. J BiolChem 1976;251:813–9
[54] Labar G, Bauvois C, Borel F, FerrerJL,Wouters J, Lambert DM. Crystal structure of the human monoacylglycerol lipase, a key actor in endocannabinoid signaling. Chembiochem 2010;11:218–27
[55] Schlosburg JE, Blankman JL, Long JZ, Nomura DK, Pan B, Kinsey SG, et al. Chronic monoacylglycerol lipase blockade causes functional antagonism of the endocannabinoid system. Nat Neurosci 2010;13:1113–9
[56] Cornaciu I, Boeszoermenyi A, Lindermuth H, Nagy HM, Cerk IK, Ebner C, Salzburger B, Gruber A, Schweiger M, Zechner R, Lass A, Zimmermann R, Oberer M. (2011) “The minimal domain of adipose triglyceride lipase (ATGL) ranges until leucine 254 and can be activated and inhibited by CGI-58 and G0S2, respectively” PLoS One. 2011;6(10):e26349.
[57] Zechner R., R. Zimmermann, T. O. Eichmann , S. D. Kohlwein , G. Haemmerle, A. Lass and F. Madeo (2012) FAT SIGNALS lipases and lipolysis in lipid metabolism and signaling. Cell. Metab. 15 : 279 – 291
[58] Kralisch, S., Klein, J.,Lossner, U., Bluher, M., Paschke, R., Stumvoll, M., and Fasshauer, M. (2005). Isoproterenol, TNFalpha, and insulin downregulate adipose triglyceride lipase in 3T3-L1 adipocytes. Mol. Cell. Endocrinol. 240, 43–49

[59] Kraemer FB, Shen WJ. Hormone-sensitive lipase: control of intracellular tri-(di-) acylglycerol and cholesteryl ester hydrolysis. J Lipid Res 2002;43: 1585–94
[60] Watt MJ, Spriet LL. Regulation and role of hormone-sensitive lipase activity in human skeletal muscle. ProcNutrSoc 2004;63:315–22
[61] Langfort J, Donsmark M, Ploug T, Holm C, Galbo H. Hormone-sensitive lipase in skeletal muscle: regulatory mechanisms. ActaPhysiolScand 2003;178: 397–403
[62] Tansey JT, Huml AM, Vogt R, Davis KE, Jones JM, Fraser KA, et al. Functional studies on native and mutated forms of perilipins. A role in protein kinase A-mediated lipolysis of triacylglycerols. J BiolChem 2003;278:8401-6
[63] Sztalryd C, Xu G, Dorward H, Tansey JT, Contreras JA, Kimmel AR, et al. Perilipin A is essential for the translocation of hormone-sensitive lipase during lipolytic activation. J Cell Biol 2003;161:1093–103
[64] Bartz, R., Zehmer, J.K., Zhu, M., Chen, Y., Serrero, G., Zhao, Y., and Liu, P. (2007). Dynamic activity of lipid droplets: protein phosphorylation and GTP- mediated protein translocation. J. Proteome Res. 6, 3256–3265
[65] Granneman, J.G., Moore, H.P., Krishnamoorthy, R., and Rathod, M. (2009). Perilipin controls lipolysis by regulating the interactions of AB-hydrolase containing 5 (Abhd5) and adipose triglyceride lipase (Atgl). J. Biol. Chem. 284, 34538–34544
[66] Miyoshi, H., Perfield, J.W., 2nd, Souza, S.C., Shen, W.J., Zhang, H.H., Stancheva, Z.S., Kraemer, F.B., Obin, M.S., and Greenberg, A.S. (2007). Control of adipose triglyceride lipase action by serine 517 of perilipin A globally regulates protein kinase A-stimulated lipolysis in adipocytes. J. Biol. Chem. 282, 996–1002
[67] M. Hochstrasser, Ubiquitin-dependent protein degradation, Annu. Rev. Genet. 30 (1996) 405–439.
[68] A. Hershko, A. Ciechanover, The ubiquitin system, Annu. Rev. Biochem. 67 (1998) 425–479.
[69] M. Hochstrasser, Ubiquitin, proteasomes, and the regulation of intracellular protein degradation, Curr.Opin. Cell Biol. 7 (1995) 215–223.
[70] L. Hicke, Protein regulation by monoubiquitin, Nat. Rev. Mol. Cell Biol. 2 (2001) 195–201.
[71] C.M. Pickart, D. Fushman, Polyubiquitin chains: polymeric protein signals, Curr. Opin. Chem. Biol. 8 (2004) 610–616.
[72] L. Waxman, J.M. Fagan, A.L. Goldberg, Demonstration of two distinct high molecular weight proteases in rabbit reticulocytes, one of which degrades ubiquitin conjugates, J. Biol. Chem. 262 (1987) 2451–2457.
[73] Rivett, A. J. (1993). Proteasomes: multicatalytic proteinase complexes. Biochemistry Journal, 291, 1–10.
[74] K. Tanaka, The proteasome: overview of structure and functions, Proc. Jpn Acad. B Phys. Biol. Sci. 85 (2009) 12–36.
[75] Petroski, M. D. (2008) The ubiquitin system, disease, and drug discovery. *BMC Biochem.*9 Suppl 1, S7
[76] Paul, S. (2008) Dysfunction of the ubiquitin-proteasome system in multiple disease conditions: therapeutic approaches. *Bioessays*30, 1172–1184
[77] Portbury A. L. (2011) Back to your heart: Ubiquitin proteasome system-regulated signal transduction. J. of Mol. and Cell. Cardiology 52 (2012) 526–537

[78] Kovsan J. (2007)Regulation of Adipocyte Lipolysis by Degradation of the Perilipin Protein**.** JBC Papers in Press DOI 10.1074/jbc.M702223200
[79]Xu G. (2005) Post-translational Regulation of Adipose Differentiation-related Protein by the Ubiquitin/Proteasome Pathway. JBC Papers in Press, DOI 10.1074/jbc.M506569200
[80] Chan S. C. (2007) Regulation of Cidea protein stability by the ubiquitin-mediated proteasomal degradation pathway. Biochem. J. 408, 259–266 doi:10.1042/BJ20070690
[81] Nian Z. (2010) Fat-specific Protein 27 Undergoes Ubiquitin-dependent Degradation Regulated by Triacylglycerol Synthesis and Lipid Droplet Formation. JBC Papers in Press, DOI 10.1074/jbc.M109.043786
[82] Boyer, P. D., Chance, B., Ernster, L., Mitchell, P., Racker, E. and Slater, E. C. (1977) Oxidative phosphorylation and photophosphorylation. Annu. Rev. Biochem. 46, 955–1026
[83] Kahn, B. B., Alquier, T., Carling, D. and Hardie, D. G. (2005) AMP-activated protein kinase: ancient energy gauge provides clues to modern understanding of metabolism. Cell Metab. 1, 15–25
[84] Carling, D. (2004) The AMP-activated protein kinase cascade: a unifying system forenergy control. Trends Biochem. Sci. 29, 18–24
[85] Hawley, S. A., Davison, M., Woods, A., Davies, S. P., Beri, R. K., Carling, D. and Hardie, D. G. (1996) Characterization of the AMP-activated protein kinase kinase from rat liver and identification of threonine 172 as the major site at which it phosphorylates AMP-activated protein kinase. J. Biol. Chem. 271, 27879–27887
[86] Tokumitsu, H. and Soderling, T. R. (1996) Requirements for calcium and calmodulin in the calmodulin kinase activation cascade. J. Biol. Chem. 271, 5617–5622
[87] Stahmann, N., Woods, A., Carling, D. and Heller, R. (2006) Thrombin activates AMP-activated protein kinase in endothelial cells via a pathway involving Ca2+ /calmodulin-dependent protein kinase kinase β.Mol.Cell.Biol. 26, 5933–5945
[88] Tamas, P., Hawley, S. A., Clarke, R. G., Mustard, K. J., Green, K., Hardie, D. G. and Cantrell, D. A. (2006) Regulation of the energy sensor AMP-activated protein kinase by antigen receptor and Ca2+ in T lymphocytes. J. Exp. Med. 203, 1665–1670
[89] Woods, A., Johnstone, S. R., Dickerson, K., Leiper, F. C., Fryer, L. G., Neumann, D., Schlattner, U., Wallimann, T., Carlson, M. and Carling, D. (2003) LKB1 is the upstream kinase in the AMP-activated protein kinase cascade. Curr. Biol. 13, 2004–2008
[90] Lage, R., Dieguez, C., Vidal-Puig, A. and Lopez, M. (2008) AMPK: a metabolic gaugeregulating whole-body energy homeostasis. Trends Mol. Med. 14, 539–549
[91]Shackelford, D. B. and Shaw, R. J. (2009) The LKB1–AMPK pathway: metabolism and growth control in tumour suppression. Nat. Rev. Cancer 9, 563–575
[92] Steinberg, G. R. and Kemp, B. E. (2009) AMPK in health and disease. Physiol. Rev. 89, 1025–1078
[93] Zhang, B. B., Zhou, G. and Li, C. (2009) AMPK: an emerging drug target for diabetes and the metabolic syndrome. Cell Metab. 9, 407–416
[94] Carling, D. (2004) The AMP-activated protein kinase cascade: a unifying system for energy control. Trends Biochem. Sci. 29, 18–24

[95] Ahmadian, M., Abbott, M.J., Tang, T., Hudak, C.S., Kim, Y., Bruss, M., Hellerstein, M.K., Lee, H.Y., Samuel, V.T., Shulman, G.I., et al. (2011). Desnutrin/ ATGL is regulated by AMPK and is required for a brown adipose phenotype. Cell Metab. 13, 739–748.
[96] Gaidhu MP, (2008) Chronic AICAR-induced AMP-kinase activation regulates adipocyte lipolysis in a time-dependent and fat depot-specific manner in rats. Journal of Lipid Research 2008, DOI 10.1194/jlr.M800480-JLR200
[97] Zierler KA, Jaeger D, Pollak NM, Eder S, Rechberger GN, Radner FP, Woelkart G, Kolb D, Schmidt A, Kumari M, Preiss-Landl K, Pieske B, Mayer B, Zimmermann R, Lass A, Zechner R, Haemmerle G. (2013) Functional cardiac lipolysis in mice critically depends on comparative gene identification-58. J Biol Chem. 2013 Feb 14. PMID: 23413028
[98] Pereira SL, Ramalho-Santos J, Branco AF, Sardão VA, Oliveira PJ, Carvalho RA. Metabolic remodeling during H9c2 myoblast differentiation: relevance for in vitro toxicity studies. CardiovascToxicol. 2011 Jun;11(2):180-90. doi: 10.1007/s12012-011-9112-4. PMID: 21431998
[99] Olzmann JA, Richter CM, Kopito RR. (2013) Spatial regulation of UBXD8 and p97/VCP controls ATGL-mediated lipid droplet turnover. ProcNatlAcadSci U S A. 2013 Jan 22;110(4):1345-50. doi: 10.1073/pnas.1213738110. Epub 2013 Jan 7. PMID: 23297223
[100] Wang X, Li J, Zheng H, Su H, Powell SR. Proteasome functional insufficiency in cardiac pathogenesis. Am J Physiol Heart Circ Physiol. 2011 Dec;301(6):H2207-19. doi: 10.1152/ajpheart.00714.2011. Epub 2011 Sep 23. Review
[101] Gaidhu, M.P., Fediuc, S., Anthony, N.M., So, M., Mirpourian, M., Perry, R.L., and Ceddia, R.B. (2009). Prolonged AICAR-induced AMP-kinase activation promotes energy dissipation in white adipocytes: novel mechanisms integrating HSL and ATGL. J. Lipid Res. 50, 704–715.
[102] Gauthier, M.S., Miyoshi, H., Souza, S.C., Cacicedo, J.M., Saha, A.K., Greenberg, A.S., and Ruderman, N.B. (2008). AMP-activated protein kinase is activated as a consequence of lipolysis in the adipocyte: potential mechanism and physiological relevance. J. Biol. Chem. 283, 16514–16524.
[103] Chakrabarti, P., English, T., Karki, S., Qiang, L., Tao, R., Kim, J., Luo, Z., Farmer, S.R., and Kandror, K.V. (2011). SIRT1 controls lipolysis in adipocytes via FOXO1-mediated expression of ATGL. J. Lipid Res. 52, 1693–170
[104] Gomes AV, Young GW, Wang Y, Zong C, Eghbali M, Drews O et al. Contrasting proteome biology and functional heterogeneity of the 20S proteasome complexes
[105] Nadia Hedhli and Christophe Depre (2010) Proteasome inhibitors and cardiac cell growth Cardiovasc Res. 2010 January 15; 85(2): 321–329. Published online 2009 July 3. doi: 10.1093/cvr/cvp226
[106] Baskin KK, Taegtmeyer H. AMP-activated protein kinase regulates E3 ligases in rodent heart. Circ Res. 2011 Oct 28;109(10):1153-61. doi: 10.1161/CIRCRESAHA.111.252742. Epub 2011 Sep 15.
[107] Quy PN, Kuma A, Pierre P, Mizushima N. Proteasome-dependent activation of mammalian target of rapamycin complex 1 (mTORC1) is essential for autophagy suppression and muscle remodeling following denervation. J Biol Chem. 2013 Jan 11;288(2):1125-34. doi: 10.1074/jbc.M112.399949. Epub 2012 Dec 3.

[108] Wing, S. S., and Goldberg, A. L. (1993) Glucocorticoids activate the ATP-ubiquitin-dependent proteolytic system in skeletal muscle during fasting. Am. J. Physiol. 264, E668–E676
[109] Tiao, G., Fagan, J. M., Samuels, N., James, J. H., Heidsen, K., Lieberman, M., Fischer, J. E., and Hasselgren, P. O. (1994) Sepsis stimulates nonlysosomal, energy dependent proteolysis and increases ubiquitin mRNA levels in rat skeletal muscle.J. Clin. Invest. 94, 2255–2264
[110] Biolo, G., Bosutti, A., Iscara, F., Toigo, G., Gallo, A., and Guarnieri, G. (2000) Contribution of the ubiquitin-proteasome pathway to overall muscle proteolysis in hypercatabolic patients. Metabolism 49, 689–691
[111] Zhang L, Tang H, Kou Y, Li R, Zheng Y, Wang Q, Zhou X, Jin L. MG132-mediated inhibition of the ubiquitin-proteasome pathway ameliorates cancer cachexia. J. Cancer Res ClinOncol. 2013 Mar 28
[112] Li J, Horak KM, Su H, Sanbe A, Robbins J, Wang X. Enhancement of proteasomal function protects against cardiac proteinopathy and ischemia/reperfusion injury in mice. J Clin Invest 121: 3689–3700, 201
[113] Powell SR, Samuel SM, Wang P, Divald A, Thirunavukkarasu M, Koneru S et al. Upregulation of myocardial 11S-activated proteasome in experimental hyperglycemia.
[114] Margret Pöschl (2009) Die Rolle von 14-3-3-Proteinen in der Regulation der Adipozyten-Triglyzeridlipase. Diplomarbeit
[115] Taschler U, Radner FP, Heier C, Schreiber R, Schweiger M, Schoiswohl G, Preiss-Landl K, Jaeger D, Reiter B, Koefeler HC, Wojciechowski J, Theussl C, Penninger JM, Lass A, Haemmerle G, Zechner R, Zimmermann R. Monoglyceride lipase deficiency in mice impairs lipolysis and attenuates diet-induced insulin resistance.
J Biol Chem. 2011 May 20;286(20):17467-77. doi: 10.1074/jbc.M110.215434.